Stem Cell Reports
Article
OPEN ACCESS

A Dominant-Negative Isoform of IKAROS Expands Primitive Normal Human Hematopoietic Cells

Philip A. Beer,[1] David J.H.F. Knapp,[1] Nagarajan Kannan,[1] Paul H. Miller,[1] Sonja Babovic,[1] Elizabeth Bulaeva,[1] Nima Aghaeepour,[1] Gabrielle Rabu,[1] Shabnam Rostamirad,[1] Kingsley Shih,[1] Lisa Wei,[1] and Connie J. Eaves[1,*]
[1]Terry Fox Laboratory, British Columbia Cancer Agency and University of British Columbia, Vancouver, BC V5Z 1L3, Canada
*Correspondence: ceaves@bccrc.ca
http://dx.doi.org/10.1016/j.stemcr.2014.09.006

SUMMARY

Disrupted IKAROS activity is a recurrent feature of some human leukemias, but effects on normal human hematopoietic cells are largely unknown. Here, we used lentivirally mediated expression of a dominant-negative isoform of IKAROS (IK6) to block normal IKAROS activity in primitive human cord blood cells and their progeny. This produced a marked (10-fold) increase in serially transplantable multipotent IK6$^+$ cells as well as increased outputs of normally differentiating B cells and granulocytes in transplanted immunodeficient mice, without producing leukemia. Accompanying T/natural killer (NK) cell outputs were unaltered, and erythroid and platelet production was reduced. Mechanistically, IK6 specifically increased human granulopoietic progenitor sensitivity to two growth factors and activated CREB and its targets (c-FOS and Cyclin B1). In more primitive human cells, IK6 prematurely initiated a B cell transcriptional program without affecting the hematopoietic stem cell-associated gene expression profile. Some of these effects were species specific, thus identifying novel roles of IKAROS in regulating normal human hematopoietic cells.

INTRODUCTION

The IKAROS transcription factor is essential for normal mouse lymphopoiesis, and its suppression by dominant-negative isoforms produces T cell tumors (Payne and Dovat, 2011). In human cells, the IK6 dominant-negative isoform has been reported to inhibit erythroid and B cell production (Dijon et al., 2008; Tonnelle et al., 2001; Tonnelle et al., 2009) and to produce an acute leukemia in cord blood cells cotransduced with a virus encoding BCR-ABL1 (Theocharides et al., 2014). A greater understanding of the role of IKAROS in the human blood system is of particular interest given the high frequency of inactivating mutations in *IKZF1* (encoding IKAROS) in human B cell leukemias as well as occasional myeloid malignancies (Grossmann et al., 2011; Jäger et al., 2010; Mullighan et al., 2008; Nacheva et al., 2013; Nakayama et al., 1999).

Here, we show that lentiviral-mediated expression of IK6 has different effects on primitive mouse and human hematopoietic cells. In mice, B-lineage outputs were suppressed and myeloid and T cells were increased, culminating occasionally in T cell leukemia. In contrast, we find that primitive human cord blood (CB) cells transduced with the same vector produce increased numbers of myeloid and B-lineage cells as well as cells able to repopulate secondary recipient mice for more than 7 months but show neither a change in T cell output nor any evidence of leukemogenesis. Together, these findings point to an ability of IKAROS to regulate primitive stages of human hematopoiesis.

RESULTS

Construction and Validation of an IK6 Lentiviral Vector

To analyze the effects of disrupting IKAROS activity in hematopoietic cells, we created two similarly high-titer lentivirus preparations: one encoding GFP plus IK6 (lacking all four DNA-binding motifs but retaining the IKAROS protein-protein interaction domain; Figure 1A), and another control virus encoding yellow fluorescent protein (YFP) only. We then transduced separate aliquots of lineage$^-$ SCA-1$^+$KIT$^+$ (LSK) adult mouse bone marrow (BM) cells with each virus and cotransplanted paired aliquots of these cells without further selection (1.5×10^4 of each/recipient) into four congenic B6-W^{41}/W^{41} (W41) and four allogeneic nonobese diabetic/severe combined immunodeficiency (NOD/SCID) interleukin-2 receptor, γ chain null (NSG) mice. Both types of recipient showed enhanced T cell and granulocyte-macrophage/monocyte (GM) outputs but transiently suppressed B cell outputs from the IK6-transduced cells (Figures S1A–S1C available online). After 24 weeks, all BM cells harvested from each primary NSG mouse were transplanted into two secondary NSG mice. These secondary mice showed a continuing enhanced output of IK6$^+$ cells (Figures S1E and S1F). In three mice, a serially transplantable and fatal IK6$^+$ (GFP$^+$) T cell leukemia developed. These findings confirm the expected T-leukemogenic activity of our IK6 vector in transduced mouse hematopoietic cells and reveal its ability to enhance normal mouse GM, but not B cell, production.

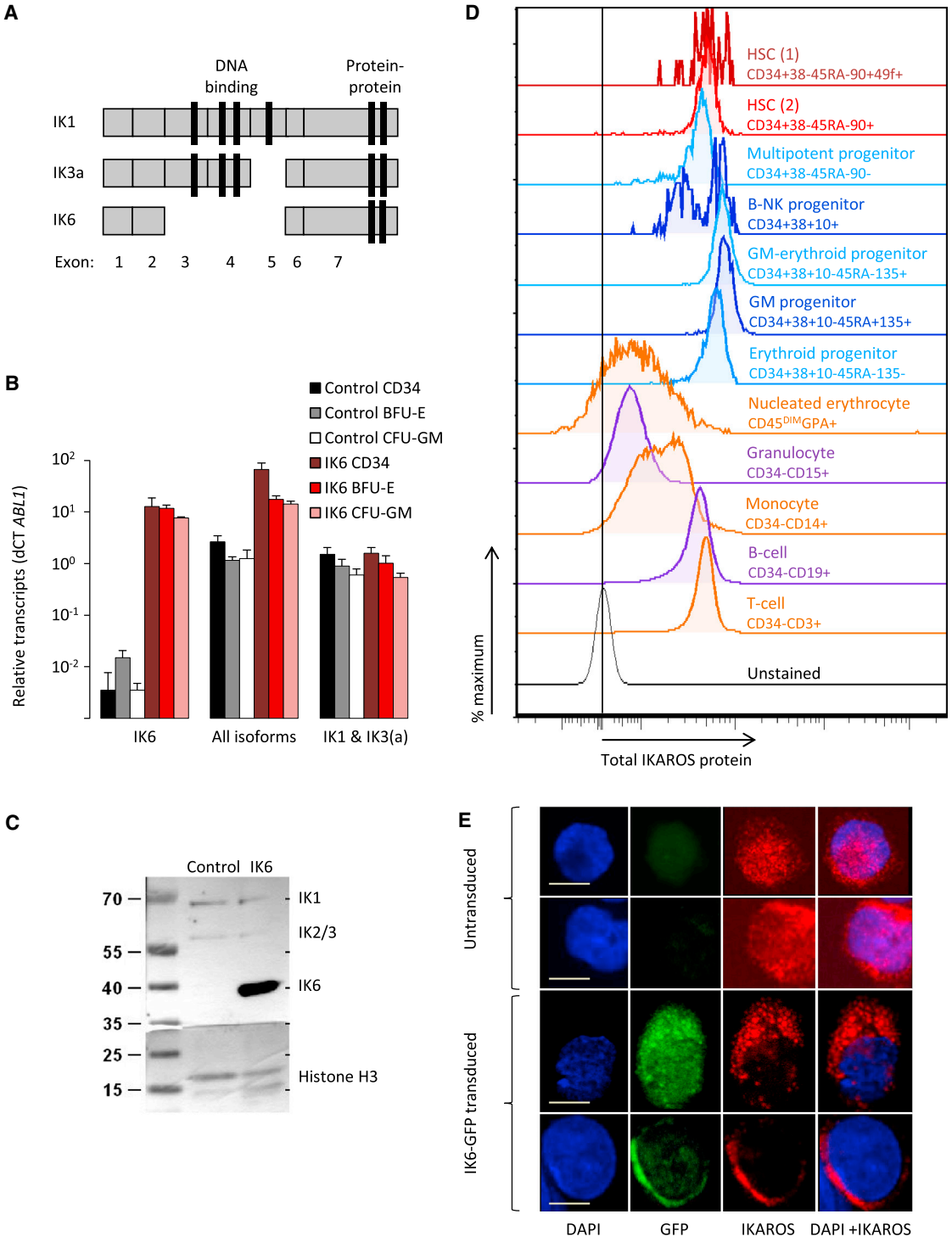

Figure 1. IKAROS Expression and Inhibition by IK6 in Human CB Cells

(A) Human IKAROS exon structure.

(B) Isoform-specific *IKZF1* transcripts determined by qRT-PCR in IK6- and control-transduced $CD34^+$ CB cells and their clonally derived erythroid (from BFU-E) and GM progeny (from CFC-GM; mean ± SEM; three experiments).

(legend continued on next page)

Transduction of human $CD34^+$ CB cells consistently yielded ~40% IK6- (GFP^+) and control-transduced (YFP^+) cells with a robust and specific increase in IK6 transcripts in the derived GFP^+ cells (Figure 1B). Western blot analysis confirmed expression of the correct size of IK6 protein at a 3-fold higher level than wild-type IKAROS proteins in the same cells (Figure 1C). Flow cytometric analyses of unmanipulated human CB cells indicated readily detectable levels of IKAROS protein in $CD34^+CD38^-CD45RA^-CD90^+CD49f^+$ cells, the most highly enriched hematopoietic stem cell (HSC)-containing CB subset thus far described (Notta et al., 2011). These levels of IKAROS remained unchanged until they decreased markedly upon entry into the terminally differentiating neutrophil and erythroid compartments (Figure 1D). Confocal image analyses demonstrated the expected punctate nuclear localization of IKAROS in normal CB $CD34^+$ cells and its absence from the nucleus in their IK6-transduced counterparts (Figure 1E). The aberrant cytoplasmic retention of IKAROS protein seen in the IK6-transduced CB cells is typical of primary $IK6^+$ leukemias (Iacobucci et al., 2008; Sun et al., 1999) and, together with the mouse leukemogenic activity of our IK6 virus, validates its expected dominant-negative effects.

IK6 Exerts Species-Specific Effects on Human Hematopoietic Cells Produced in Transplanted Mice

To examine the effects of IK6 on human hematopoietic cells, we used a similar cotransplant strategy in which IK6- and control-transduced $CD34^+$ CB cells were coinjected into both NSG mice and NSG mice producing human interleukin-3 (IL-3), GM colony-stimulating factor (GM-CSF), and Steel factor (SF) (NGS-3GS mice; Figure 2A). Measurement of *IKZF1* transcripts and intracellular IKAROS protein levels in different subsets of GFP^+ human $CD34^+$ cells isolated from these mice confirmed their continuing specific and high-level expression of the IK6 transgene (Figures 2B and 2C).

At 8–10 weeks posttransplant, the BM and spleens of both types of recipient contained 5- to 10-fold more human $CD45^+$ cells derived from IK6- (GFP^+) as compared to control-transduced (YFP^+) cells ($p < 0.01$; Figure 2D). However, the IK6-mediated increase in human cell production in this system was due to different lineage-specific effects than those seen with mouse cells. Specifically, in contrast to the IK6-mediated decrease in mouse B cell outputs (Figure S1), IK6 caused a 13 ± 3-fold increase in human B-lineage ($CD19^+$) cell production, without any detectable alteration in their stepwise differentiation (as indicated by similarly enhanced ratios of IK6- to control-derived human cells down to the stage of surface immunoglobulin M^+ B cell production; Figures 2E and 2F). Also in contrast to the transduced mouse cells, IK6 had no detectable effect on the output of human $CD3^+$ (T) cells, including $CD45RO^+$ (memory) and $CD45RA^+$ (naive) T cell subsets (Figures 2F and S2), or human $CD3^-CD56^+$ (natural killer [NK]) cells. Nevertheless, the in vivo output of $CD33^+$ (GM) cells from IK6-transduced human CB cells was significantly enhanced (Figures 2E and 2F), as also seen in the mouse experiments (Figure S1). Recipients of transduced human CB cells also showed a decreased number of circulating platelets derived from the IK6-transduced cells as compared to controls (Figure 2G). The same was the case for the erythroid (but not the GM) colony-forming cells (CFCs) in the $CD34^+CD38^+CD45RA^-FLT3^+$ cells isolated from the BM of the mice (Figure 2H). These results are of interest, in light of previous data suggesting normal IKAROS activity is required for mouse and human erythropoiesis but acts as a negative regulator of mouse megakaryopoiesis (Dijon et al., 2008; Lopez et al., 2002; Malinge et al., 2013).

Together, these findings show that IK6 has selective, rapid, and species-specific effects on the outputs of different lineages produced in vivo (in transplanted immunodeficient mice) from transduced human $CD34^+$ CB cells.

IK6-Enhances the Long-Term In Vivo Expansion of Primitive Human Hematopoietic Cells but Is Not Leukemogenic

In the human CB transplant experiments, we found the progeny of IK6-transduced cells were more prominent in all primitive ($CD34^+$) human phenotypes examined 10 weeks posttransplant (including lymphoid- and myeloid-restricted as well as lymphomyeloid progenitors; Figure 2I). Secondary transplants of pooled BM cells harvested from three of the 10-week primary mice were then performed (equivalent to one primary mouse, comprising cells from two femurs, two tibiae, and the pelvis, per secondary recipient). Ten weeks later, none of these secondary mice contained detectable progeny of the control-transduced cells (<0.01% YFP^+ chimerism). In contrast, GFP^+ progeny of the IK6-transduced cells, including $CD34^+$, GM, B, T, and NK cells, were readily detectable in all three secondary mice (0.2%–7% BM chimerism).

In a second, similarly designed, human CB transplant experiment, significantly higher outputs from IK6-transduced cells were maintained for 6 months compared with

(C) IKAROS protein isoforms in $CD34^+$ CB cells analyzed by western blotting with histone H3 as the loading control.
(D) Representative flow cytometric profiles of intracellular IKAROS in normal human CB cell subsets (from one of three experiments).
(E) Confocal microscopy images of representative single untransduced or IK6-transduced $CD34^+$ CB cells stained with DAPI (blue) and an antibody reactive with both full-length IKAROS and IK6 (red). Scale bar, 10 μm.

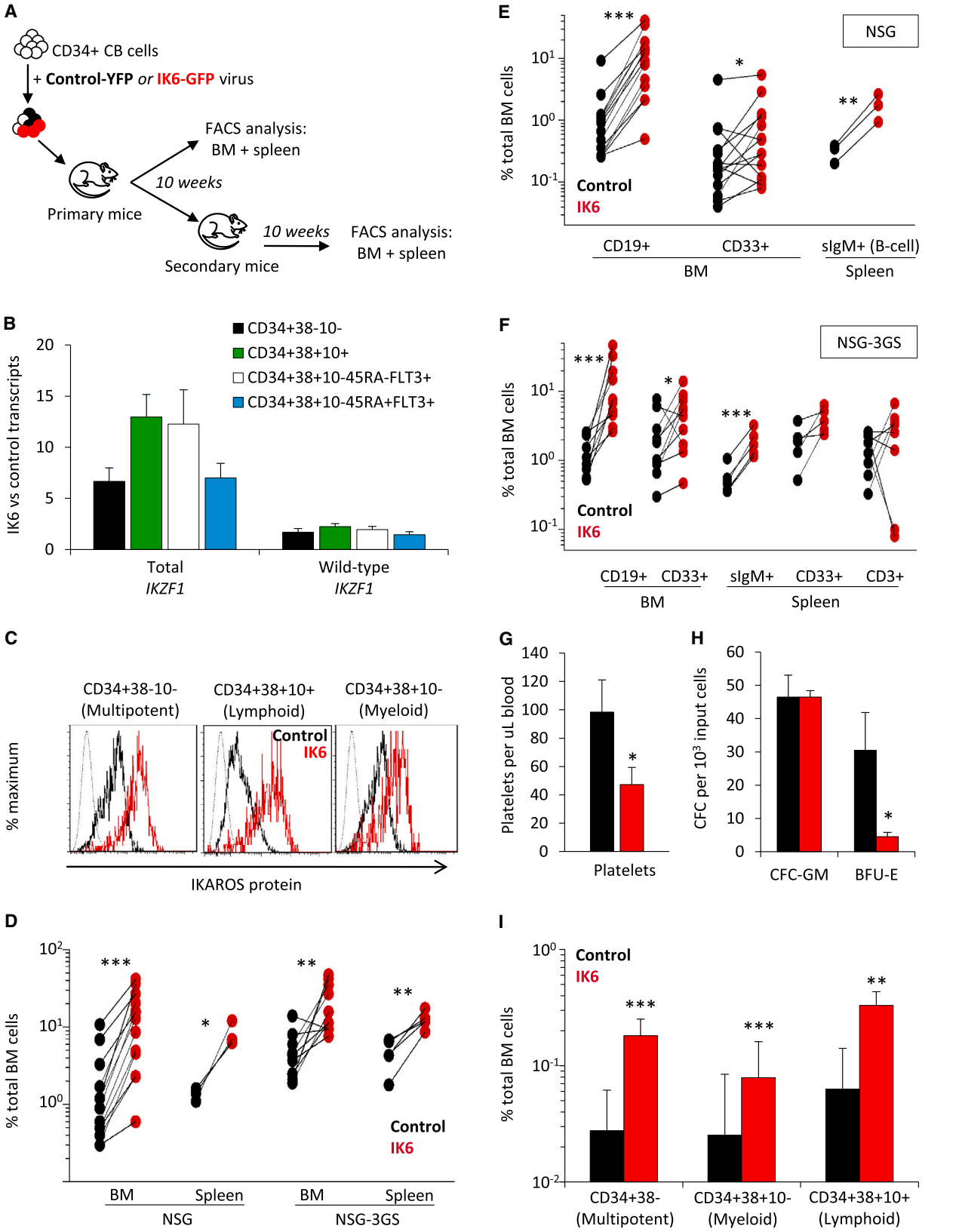

(legend on next page)

controls, including a greater content of IK6$^+$ cells in different CD34$^+$ subsets as well as the B and GM lineages (Figures 3A and 3B). To assess the regenerative activity of the more primitive cells, we isolated the human CD34$^+$CD38$^-$ cells from the 6-month primary mice and transplanted the equivalent of 18% or 90% of the cells present in one primary mouse (obtained from two femurs, two tibiae, and the pelvis) into each secondary mouse. These secondary recipients again showed a significantly greater content of IK6$^+$ as compared to control cells another 10 weeks later (Figure 3C), and the proportion engrafted with human IK6$^+$ cells was also higher (Figure 3D). The absolute numbers of 10-week human lymphomyeloid repopulating cells regenerated in the primary mice calculated from these data revealed a 10-fold higher number of those derived from the IK6-transduced cells (IK6 = 1.5 versus control $\leq$ 0.15, p = 0.0003; Figure 3E). Analysis of the same secondary mice another 20 weeks later (i.e., 30 weeks posttransplant) reinforced this difference in the ability of IK6 to enhance the regeneration in vivo of human cells with very-long-term multipotent repopulating activity (Figure 3F). Notably, even after the full 60 weeks of follow-up through two serial transplants, there was no evidence of leukemia in any mice.

Together, these studies provide definitive evidence of a marked stimulatory, but nontransforming, effect of IK6 on the regeneration in vivo of very primitive human hematopoietic cells.

IK6 Has Direct and Opposite Effects on Human GM and Erythropoietic Progenitors

Direct transduction of either early (CD34$^+$CD38$^-$) or late-stage (CD34$^+$CD38$^+$FLT3$^+$CD45RA$^{+/-}$) phenotypically defined GM progenitors with IK6 did not alter their frequency of GM colony formation in vitro (Figures S3A and S3B) or the size of clones generated (Figure S3C). In contrast, despite a similar level of expression of IK6 transcripts in the differentiated erythroid and GM cells ultimately obtained, direct transduction of every stage of erythroid progenitor selectively reduced the clonogenic activity of the IK6$^+$ cells (Figures S3D and S3E). Although the erythroid colonies generated from IK6-transduced cells did not appear obviously altered in size, morphology, or hemoglobinization, flow cytometric analysis showed they contained an increased proportion of CD71$^{\pm}$GPA$^-$ (immature) erythroblasts and a reduced content of CD71$^-$GPA$^+$ (more mature) erythroid cells compared to controls (Figures S3F and S3G). Consistent with these finding was the reduced expression of two genes critical to erythroid cell maturation (*NFE2* and *GATA1*) in the IK6-derived erythroid colonies (Figure S3H).

To examine effects on earlier stages of granulopoiesis, we compared the output of GM-lineage cells for up to 6 weeks in long-term cultures (LTCs) (Hogge et al., 1996) modified to include mouse fibroblasts engineered to produce human FLT3-ligand (FL) as well as G-CSF, SF, and IL-3 (Figure 4A). The FL-producing feeders were included because we have found this improves CFC-GM outputs from primitive subsets of CD34$^+$ CB cells cultured for $\geq$6 weeks under these conditions (M. Liu, A. Cheung, D.J.H.F.K., K. Lucke, S. Imren, Y. Zhao, V. Lecault, D.E. Hogge, J. Piret, C. Hansen, R.K. Humphries, and C.J.E., unpublished data). After 4 weeks, the nonadherent populations in these LTCs consisted almost exclusively of terminally differentiated monocytes and neutrophils (Figure 4B), with a greater contribution from the IK6-expressing cells than from the control-transduced cells (Figure 4C). We also detected a slightly (but significantly [p < 0.01]) reduced frequency of nonviable cells in the mature (nonadherent) IK6$^+$ cells (Figure 4D). Fortnightly assessment of the CFC-GM content of these LTCs showed that ~3-fold more were produced from the IK6-transduced cells, although this increase did not

Figure 2. Enhanced Multilineage Repopulating Activity of IK6-Transduced Human CD34$^+$ CB Cells

(A) Experimental design.

(B) Ratio of *ABL1/B2M* normalized *IKZF1* transcript levels in transduced CD34$^+$ human cell subsets generated in NSG mice (mean ± SEM, four mice).

(C) Representative flow cytometric profiles of total IKAROS protein in human cells generated in five NSG mice (dotted line shows unstained control).

(D) Paired comparisons of total IK6- and control-derived human CD45$^+$ cells in individual mice transplanted 8–10 weeks previously (24 mice from five cohorts).

(E and F) Ten-week posttransplant levels of human CD19$^+$ and surface immunoglobulin M$^+$ (B), CD3$^+$ (T), and CD33$^+$ (GM) cells in the same mice shown in (D).

(G) Platelet levels in the blood of NSG mice transplanted 4–10 weeks previously (mean ± SEM; seven mice from two cohorts).

(H) Colonies derived from equal numbers of IK6- and control-transduced myeloerythroid progenitors sorted from the BM of NSG mice transplanted 10 weeks previously (mean ± SEM; three mice).

(I) Levels of different human CD34$^+$ subsets in the BM of primary NSG mice transplanted 10 weeks previously (mean ± SEM, 14 mice).

Progenitor-enriched fractions: multipotent, CD34$^+$CD38$^-$; lymphoid, CD34$^+$CD38$^+$CD10$^+$; myeloerythroid, CD34$^+$CD38$^+$CD45RA$^-$FLT3$^+$; granulopoietic, CD34$^+$CD38$^+$CD45RA$^+$FLT3$^+$. BFU-E, burst-forming unit-erythroid; CFC-GM, colony-forming cell-GM. *p < 0.05; **p < 0.01; ***p < 0.001. See also Figure S2.

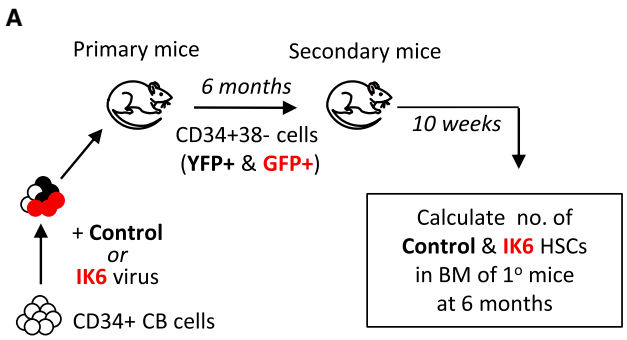

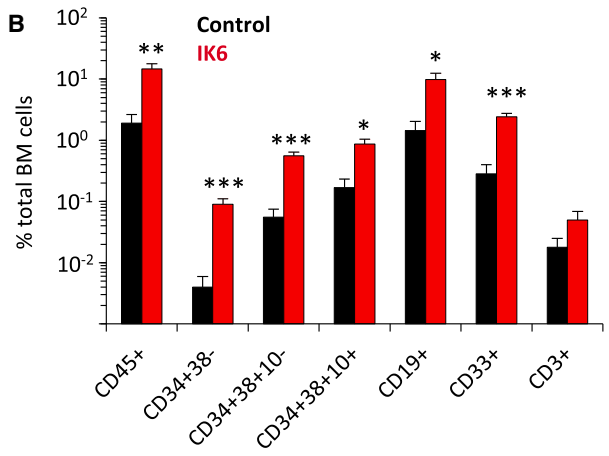

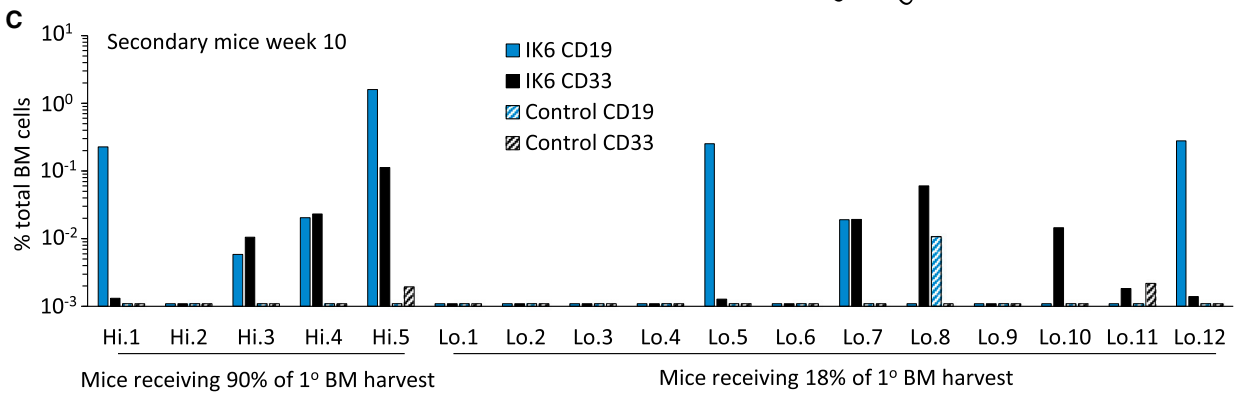

D

Dose of 1° BM cells/2° mouse (% of a 1° BM harvest)	No. of bilineage +ve 2° mice / no. of 2° mice tested
18	0/12 for control cells
18	3/12 for IK6 cells
90	0/5 for control cells
90	4/5 for IK6 cells

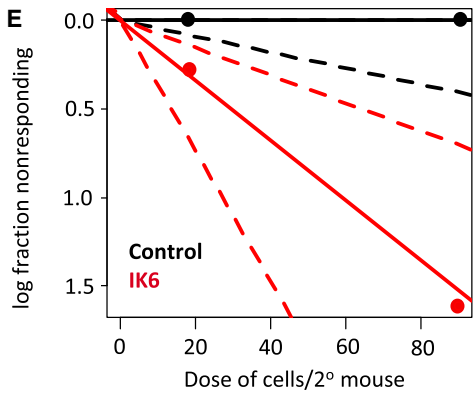

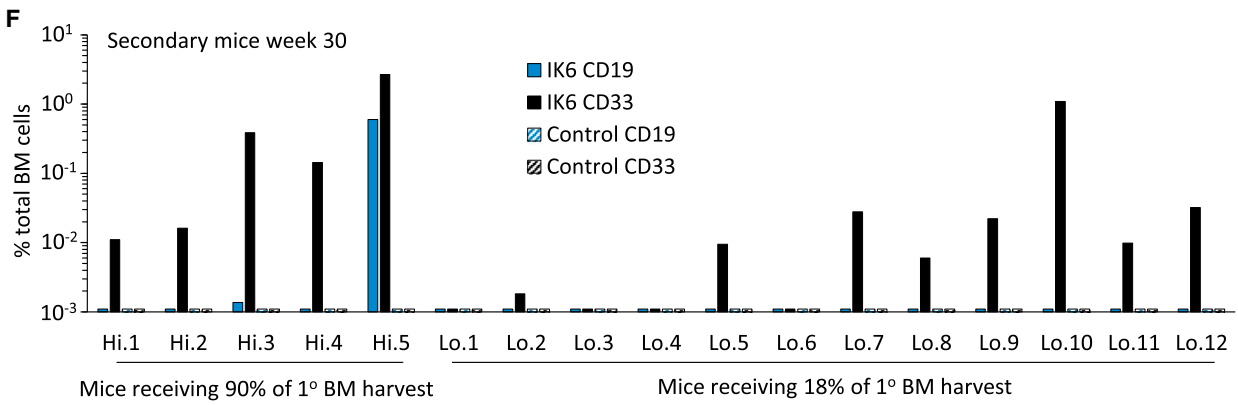

(legend on next page)

become apparent until the sixth week (Figure 4E). By this time, the total number of IK6-derived $CD34^+$ cells in the cultures was also ~3-fold higher than controls (Figure 4F). Interestingly, the increase in total cells was preceded by a small but statistically significant reduction of apoptotic (cleaved caspase-3^+) cells in the IK6-expressing $CD34^+$ population present in 4- to 5-week LTCs (Figure 4G).

To define more precisely which GM progenitors can be functionally affected by expression of IK6, we examined the serial output of CFC-GMs in stroma-free growth factor-supplemented suspension cultures initiated with different subsets of directly transduced $CD34^+$ CB cells. Primitive $CD34^+CD38^-$ (lymphomyeloid-enriched) progenitors produced a late and significant increase in CFC-GMs (Figure 4H) that was not seen when IK6 was introduced into the more differentiated $CD34^+CD38^+$ $CD45RA^-FLT3^+$ (myeloerythroid-enriched) progenitors (Figure 4I), although a transiently increased CFC-GM output was seen in cultures initiated with the even later IK6-transduced $CD34^+CD38^+CD45RA^+FLT3^+$ cells (which consist mainly of CFC-GMs) (Figure 4J).

Together, these findings point to an ability of IK6 to strongly enhance the generation of primitive human GM progenitors, with a potential modulation of their survival but little effect on their subsequent differentiation. This contrasts with the marked inhibitory effect that IK6 exerts on human erythropoietic and platelet precursors.

IK6 Sensitizes Human GM Progenitors Selectively to GM-CSF and IL-3

To investigate mechanism(s) by which IK6-mediated suppression of IKAROS in CB cells may enhance production of GM progenitors and/or their more primitive precursors, we examined the 6-week outputs of cells in separate LTCs containing FL-producing feeders to which IL-3, GM-CSF, G-CSF, SF, or IL-5 was then added individually as part of the weekly medium exchange. The addition of either GM-CSF or IL-3, but not G-CSF, SF, or IL-5, had a marked enhancing effect on cell outputs from $IK6^+$ cells as compared to controls (Figure 5A). Flow cytometric analysis of the cells present in 6-week cultures to which GM-CSF or IL-3 was added did not show any alteration in GM-CSF or IL-3 receptor expression on any primitive or mature cell subpopulation (data not shown). However, CFC-GM assays of freshly transduced $CD34^+$ cells demonstrated that IK6 expression rendered them more sensitive to either GM-CSF- or IL-3-stimulated colony formation (Figures 5B and 5C). This occurred in the absence of any evidence of autocrine GM-CSF or IL-3 production (based on the absence of both transcripts by quantitative RT-PCR [qRT-PCR] and secreted protein by ELISA; data not shown). Thus, the enhanced GM-cell output from IK6-transduced $CD34^+$ CB cells appears to be mediated, at least in part, by cell-intrinsic changes that sensitize their responses to GM-CSF and IL-3 in ways that do not affect responses to FL, SF, G-CSF, or IL-5.

Given that IK6-transduced mouse LSKs also showed enhanced granulopoiesis in vivo, we asked whether this might also be associated with an increased sensitivity to IL-3. However, the outputs from IK6- and control-transduced mouse progenitors were equivalent across a wide range of IL-3 dilutions (Figure S4), indicating a species-specific effect of IK6 in enhancing the IL-3 sensitivity of human cells.

IK6 Activates CREB and Its Downstream Targets FOS and Cyclin B1

Intracellular flow cytometric analysis of mature ($CD34^-$ $11b^+$) myeloid cells isolated from LTCs showed that pre- (basal), and post-GM-CSF- or IL-3-activated levels of phospho-CREB were higher in the progeny of IK6-transduced cells as compared to controls, although the levels of phospho-STAT3 and phospho-STAT5 were not consistently different (Figure 5D). A more comprehensive analysis of $CD34^+$ cells from the same LTCs also showed no difference in basal JAK-STAT pathway activity in the IK6-transduced cells but revealed consistently higher basal activation of several other key signaling elements, including CREB and members of the RAS pathway (Figure 5E). After GM-CSF or IL-3 stimulation, peak levels of phosphorylated

Figure 3. IK6 Enhances the In Vivo Expansion of Multipotent Repopulating Human CB Cells

(A) Experimental design.

(B) Different subsets of IK6- and control-derived human cells in the BM of primary NSG mice 26 weeks posttransplant (mean ± SEM; eight mice).

(C) Levels of human $CD19^+$ (B) and $CD33^+$ (GM) cells derived from IK6- and control transduced cells in the BM of individual secondary NSG mice transplanted 10 weeks previously. Limit of detection = 0.0001% based on analyses of $\geq 10^6$ live cells.

(D) Frequency of secondary mice dually repopulated with control- or IK6-transduced human lymphoid and myeloid cells.

(E) Plot of data shown in (D), generated using the ELDA algorithm (Hu and Smyth, 2009), showing the natural log fraction of the nonengrafted (nonresponding) mice plotted on a linear scale on the y axis versus the transplant cell dose on the x axis.

(F) Levels of human $CD19^+$ (B) and $CD33^+$ (GM) cells derived from control- and IK6-transduced cells in the BM of individual secondary NSG mice transplanted 30 weeks previously.

*$p < 0.05$; **$p < 0.01$; ***$p < 0.001$.

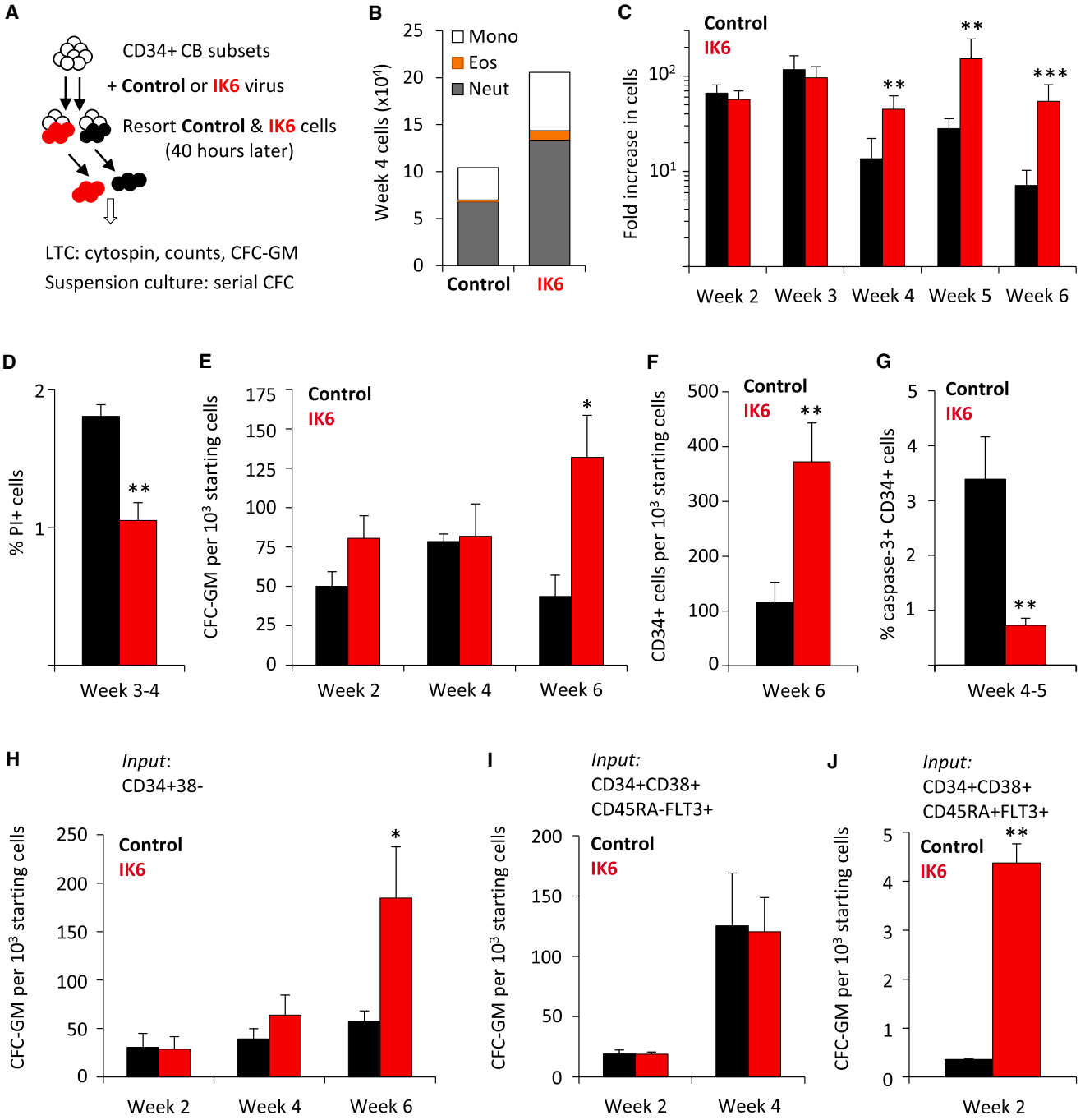

Figure 4. IK6 Enhances GM Outputs at Multiple Stages of GM Progenitor Differentiation

(A) Experimental design.

(B) Numbers of mature cell types in the nonadherent fraction of 4-week-old LTCs (200 cells assessed/sample; three experiments).

(C) Kinetics of the enhancing effect of IK6 on LTC cell outputs (mean ± SEM; three experiments).

(D) Proportion of PI^+ nonadherent IK6- and control-transduced cells in 3- to 4-week-old LTCs (mean ± SEM; three experiments).

(E) Total CFC-GMs derived from IK6- and control-transduced cells in LTCs (mean ± SEM; three experiments).

(F) Total $CD34^+$ cells derived from IK6- and control-transduced cells in 6-week LTCs (mean ± SEM; three experiments).

(legend continued on next page)

CREB were also significantly higher in the $CD34^+$ progeny of IK6-transduced cells (Figure 5F and data not shown). This greater activation of CREB was evident over a range of GM-CSF concentrations (Figure 5G).

Previous studies have linked CREB activation to cell cycle control (Zhang et al., 2005). To investigate whether IK6 expression was associated with altered expression of cell cycle regulators, we surveyed a number of candidates. The results showed *FOS*, *CCNA2* and *CCNB1* transcripts to be significantly higher in subsets of $CD34^+$ cells derived in vitro (in LTCs) from IK6-transduced cells as compared to controls (Figure 6A). FOS protein was also significantly more abundant in $CD34^+$ cells generated in vitro from IK6-transduced cells with a mean fluorescence intensity (MFI) value for $IK6^+$ cells of 209 ± 11 versus 175 ± 15 for controls ($p = 0.01$; Figure 6B). Extension of these analyses to primitive subsets generated in xenografted mice again revealed significantly higher levels of phospho-CREB in IK6-derived $CD34^+CD38^+CD10^-$ (early myeloid) as well as $CD34^+CD38^+CD10^+$ (early lymphoid) cells (Figure 6C). Intracellular levels of FOS were also higher in the early myeloid, but not the early lymphoid, cells obtained from the same mice (Figure 6D). In addition, we found that a higher proportion of the IK6-derived early myeloid and lymphoid cells stained positively for Cyclin B1 (Figures 6E and 6F). These findings identify CREB and its targets, FOS and Cyclin B1, as candidate deregulated mediators of the effects of IK6 effects in human hematopoietic cells.

IK6 Prematurely Activates a B Cell Transcriptional Program in Transduced Human $CD34^+CD38^-$ Cells

Examination of the levels of expression of candidate IKAROS target genes (Ferreirós-Vidal et al., 2013; Ma et al., 2010; Ross et al., 2012; Zhang et al., 2012) in IK6-transduced human progenitor subsets isolated from repopulated mice revealed *CCND2* transcripts (encoding the cell-cycle regulator Cyclin D2) to be elevated in $CD34^+CD38^+CD10^+$ (early lymphoid) cells, but not in other $CD34^+$ subset (Figure 7A). However, we did not detect any effects on the expression of other genes assessed in these experiments, which included *MYC* and *CDKN1B* (encoding p27). These findings suggest that Cyclin D2 may play a role in the IK6-induced expansion of human lymphoid progenitors, but not their multipotent or myeloid counterparts.

Transcriptome-wide gene expression data were obtained by analysis of human $CD34^+CD38^-$ cells sorted from three mice transplanted 10 weeks earlier with transduced $CD34^+$ CB cells. KEGG database interrogation identified 26 upregulated pathways (14%) and nine downregulated pathways (5%) in the $IK6^+$ cells as compared to control cells (threshold: $q < 0.1$; Table S1). Notably, more than half the pathways upregulated in the $IK6^+$ cells were related to signaling or cancer (31% and 23%, respectively). Further interrogation of this transcriptome data set for possible differential enrichment of genes harboring computationally derived transcription factor binding sites (using TRANSFAC data sets) identified CREB, STAT5, FOXO, E2F, and LEF1 (threshold: $q < 0.1$; Table S2). In contrast, results for genes harboring MYC binding sites were equivocal (Figure 7B). A more focused analysis using lists of CREB and STAT5 target genes derived from studies of human cells (Dawson et al., 2012; Zhang et al., 2005) revealed significantly different CREB target gene expression in the $CD34^+CD38^-$ progeny of the IK6-transduced cells ($q = 0.002$; Figure 7C) but no difference in STAT5 target gene expression ($q = 0.4$).

Expression of genes harboring binding sites for the lymphoid-specific LEF1 transcription factor were found to be increased in IK6-derived $CD34^+CD38^-$ cells (Figure 7B), suggesting activation of a B-lineage differentiation program. To further investigate this possibility, we compared our data set with a set of genes that were at least 2-fold more highly expressed in normal human $CD34^+38^+10^+$ (early B-lineage) cells as compared to human multipotent (HSC-enriched) $CD34^+CD38^-$ cells (Hystad et al., 2007). This comparison demonstrated significant upregulation of the B-lineage gene set in the $IK6^+$ $CD34^+CD38^-$ cells as compared with controls ($q = 0.02$; Figure 7D). In contrast, a parallel analysis of these cells for genes normally expressed at higher levels in human $CD34^+CD38^-$ cells than in later progenitors (Eppert et al., 2011; Novershtern et al., 2011) demonstrated no corresponding IK6-associated difference ($q = 0.6$ and $q = 0.7$). These findings demonstrate that IK6 initiates a B-lineage transcriptional program prematurely in $CD34^+CD38^-$ cells, without compromising the expression of an HSC transcriptional signature.

DISCUSSION

Growing evidence suggests that the mechanisms by which signaling networks regulate normal human HSC self-renewal and lineage restriction are highly complex processes that involve many genes implicated in human

(G) Proportion of cleaved caspase-3^+ $CD34^+$ cells derived from IK6- and control-transduced cells in 4- to 5-week LTCs (mean ± SEM; three experiments).
(H–J) CFC-GMs in suspension cultures initiated with different subsets of transduced $CD34^+$ CB cells (normalized to 10^3 input cells; mean ± SEM; three experiments).
*$p < 0.05$; **$p < 0.01$; ***$p < 0.001$. See also Figure S3.

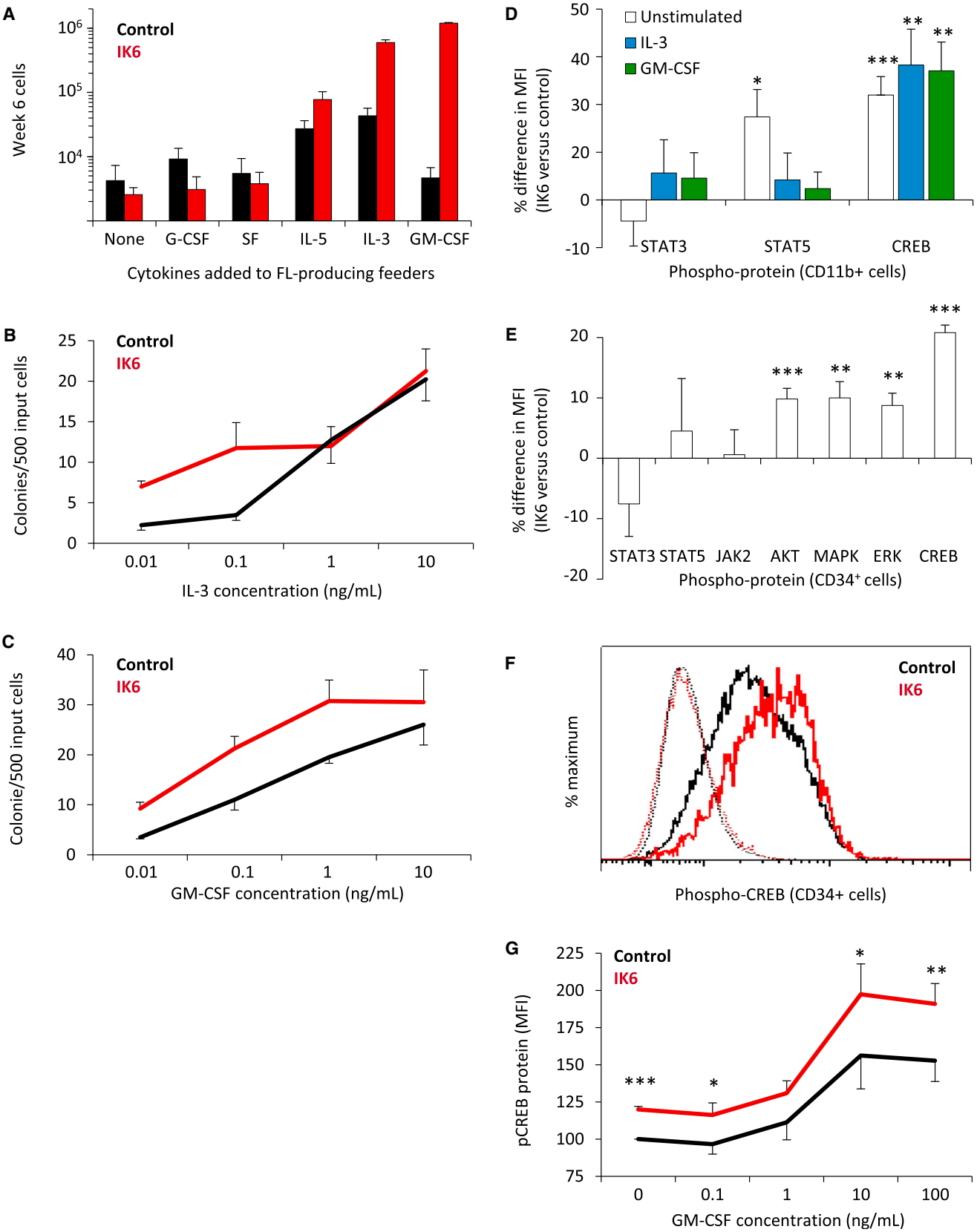

(legend on next page)

leukemogenesis. Nevertheless, the role in normal human hematopoiesis played by many of these leukemia-associated genes remains poorly understood. Much has been learned from studies of genetically manipulated mouse cells, in which the expression of genes from an endogenous promoter can be controlled both temporally and in a lineage-specific manner. However, the conclusions derived from mouse models are necessarily limited by species-specific differences (Payne and Crooks, 2007; Rangarajan and Weinberg, 2003). Fortunately, recent technical advances are making it increasingly possible to assess the consequences of direct gene manipulation in human hematopoietic cells. These include the development of lentiviral vectors that can efficiently transduce primitive human hematopoietic cell populations, improved multiparameter flow cytometry, array-based techniques applicable to small numbers of cells, and the generation of highly immunodeficient long-lived strains of mice that can reproducibly support sustained, high-level reconstitution with human hematopoietic cells (Billerbeck et al., 2011; Doulatov et al., 2012; Miller et al., 2013). Here, we exploited such methods to examine and compare the cellular and molecular consequences of IK6 in primitive normal human and mouse hematopoietic cells. In addition, we made use of an experimental design in which matched numbers of IK6- and control-transduced cells were cotransplanted into the same recipients or analyzed in the same cultures to enable a precise and accurate comparison of *absolute* (rather than *relative*) lineage contributions not necessarily otherwise possible.

The most significant finding in these studies was the 10-fold enhanced expansion of transplantable HSCs in mice engrafted with IK6-transduced human $CD34^+$ CB cells. This was indicated both by the higher numbers of $CD34^+CD38^-$ cells regenerated from the IK6-transduced cells after 6 months in primary recipients and by the functional ability of these cells to reconstitute hematopoiesis in secondary mice for another 7.5 months. To our knowledge, this effect matches or exceeds any strategy for experimentally expanding human HSCs thus far reported. It also stands in sharp contrast to the reported suppression of mouse HSC expansion by disruption of IKAROS activity (Nichogiannopoulou et al., 1999; Papathanasiou et al., 2009), thus underscoring the importance of using primary human hematopoietic cells to interrogate the role of IKAROS in their normal regulation.

Also striking was the consistent IK6-induced in vivo enhancement of human B-lineage cell generation, in contrast to the impaired B cell outputs obtained by loss of IKAROS activity in mouse cells (Joshi et al., 2014; Schwickert et al., 2014) also confirmed here. These effects of IK6 on human B cell development were presaged by the premature activation of a B-lineage transcriptional program in the human HSC-enriched $CD34^+CD38^-$ compartment, which did not interfere with their HSC activity or subsequent execution of normal B cell differentiation. We also saw different effects on mouse and human T cell outputs, which were enhanced by IK6 expression in mouse cells, consistent with previous reports, whereas human T cell outputs were unaffected. Historical limitations inherent to previous human modeling systems may explain why we did not observe the IK6-induced suppression of human B cell production previously reported in engrafted NOD/SCID mice (Tonnelle et al., 2001).

One potential explanation for the difference in effects of IK6 on mouse and human lymphopoiesis could be species-specific differences in the downstream events activated, as exemplified by the discrepancies in B cell phenotypes of human inherited immunodeficiency syndromes when compared with their equivalent mouse models (Conley et al., 2000; Mestas and Hughes, 2004). Dominant-negative isoforms may also differentially suppress wild-type IKAROS activity in the different models thus far described, raising the interesting possibility that the antiproliferative and pro-B-lineage differentiation roles of IKAROS may not be tightly linked.

Figure 5. IK6 Sensitizes Human GM Progenitors to GM-CSF and IL-3

(A) Effect of different human growth factors on 6-week cell outputs from IK6- and control-transduced human cells (mean ± SEM; four replicates each from two experiments).

(B and C) IL-3 and GM-CSF dose-response relationships for GM colony formation from IK6- and control-transduced human $CD34^+$ cells (mean ± SEM; two replicates each from two experiments).

(D) Differences in levels of intracellular phosphoproteins in IK6- versus control-derived $CD34^-11b^+$ GM cells stimulated (or not) with GM-CSF or IL-3 (mean ± SEM of MFI ratios; six to eight experiments).

(E) Basal levels of intracellular phosphoproteins in IK6- versus control-derived $CD34^+$ cells (mean ± SEM of MFI ratios from six to eight experiments).

(F) Representative flow cytometric profiles of phospho-CREB levels (solid lines) in IL-3-stimulated $CD34^+$ cells derived from IK6- and control-transduced cells. Dotted lines show staining in the absence of the phospho-CREB antibody.

(G) Phospho-CREB response of $CD34^+$ cells derived from IK6- and control-transduced cells to increasing concentrations of GM-CSF (mean ± SEM for normalized changes in phospho-CREB MFI values, four experiments).

MFI, median fluorescence intensity; FL, FLT3-ligand. *$p < 0.05$; **$p < 0.01$; ***$p < 0.001$.

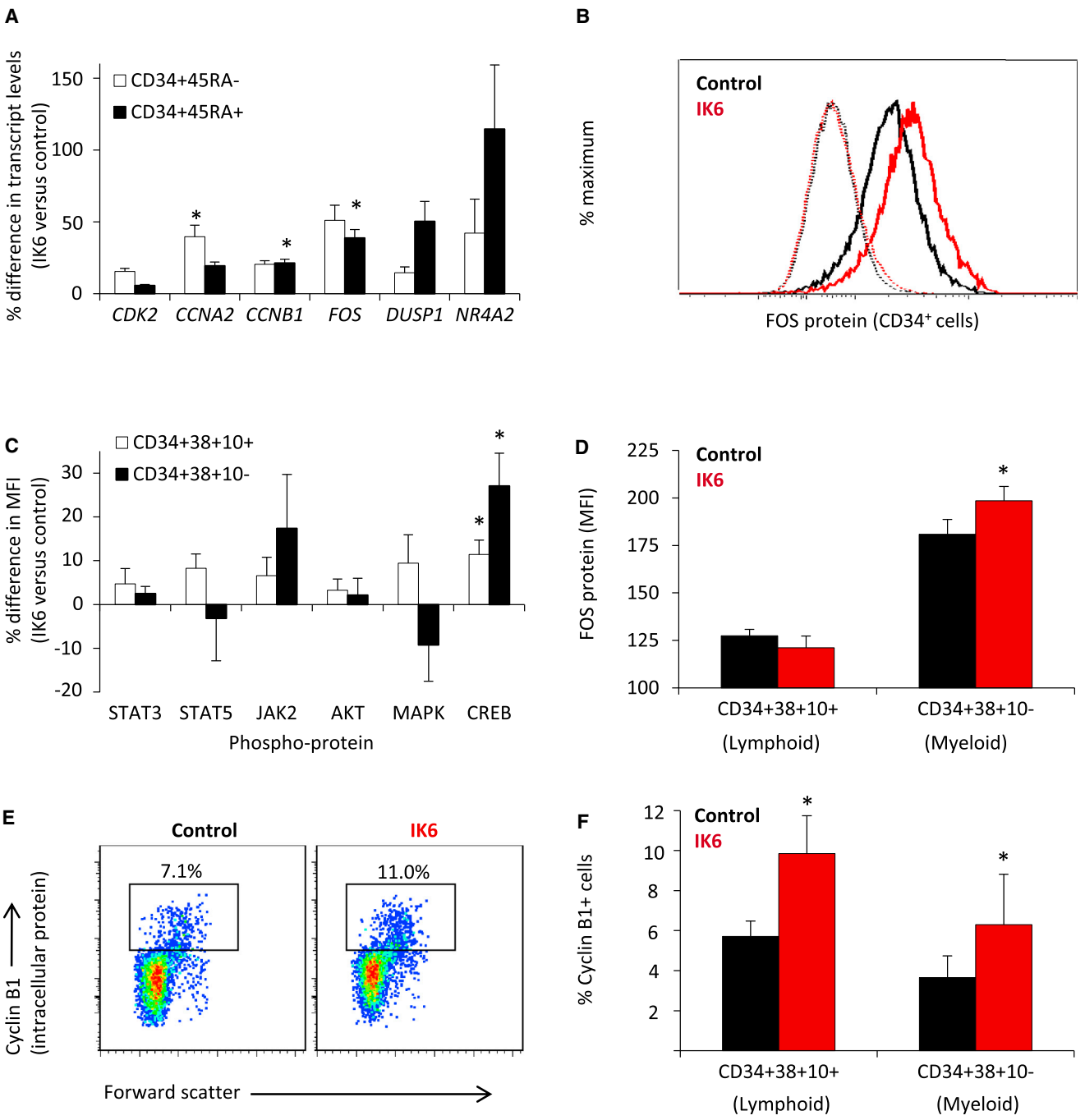

Figure 6. IK6 Activates CREB and Its Targets FOS and Cyclin B1 in CD34$^+$ Human CB Cells

(A) IK6-stimulated gene expression in subsets of CD34$^+$ cells from 3- to 4-week LTCs (mean ± SEM ratio of normalized transcript levels; seven experiments).

(B) Representative flow cytometric profile of intracellular FOS protein levels (solid lines) in CD34$^+$ cells derived from IK6- and control-transduced cells in 3-week LTCs. Dotted lines indicate staining in the absence of anti-FOS antibody.

(C) Percentage differences in phosphoprotein levels (MFIs) in different subsets of CD34$^+$ cells generated from IK6- and control-transduced cells cotransplanted into NSG mice (mean ± SEM, four mice). Phospho-ERK was not detected.

(D) FOS protein levels in progeny of IK6- and control-transduced cells cotransplanted into NSG mice 10 weeks previously (mean ± SEM, four mice).

(legend continued on next page)

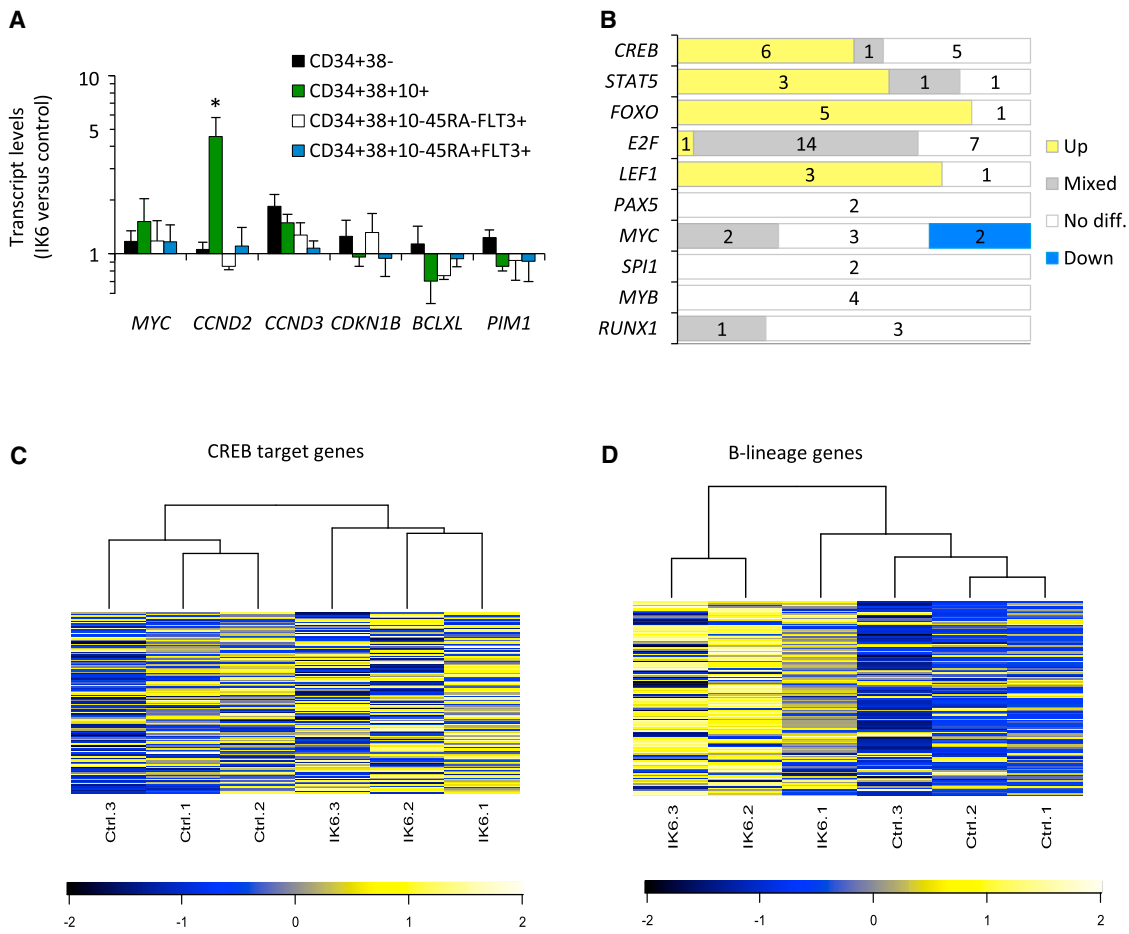

Figure 7. IK6 Activates a B-Lineage Transcriptional Program Prematurely in Human CD34$^+$CD38$^-$ Cells

(A) Normalized transcript levels in subsets of human cells generated from IK6- versus control-transduced cells in four cotransplanted NSG mice (mean ± SEM).

(B) Differential enrichment of genes bearing specific transcription factor binding sites in a comparison of gene expression data from the CD34$^+$CD38$^-$ progeny of IK6- and control-transduced cells sorted from transplanted mice. "Up" indicates a positive enrichment. "Down" indicates a negative enrichment. "Mixed" indicates enrichment including both up- and downregulated genes.

(C) Unsupervised clustering and heatmap of human CREB target genes (500 genes showing strongest CREB binding in a chromatin immunoprecipitation sequencing study of human cells; Zhang et al., 2005) showing relative expression (*Z* score) in CD34$^+$CD38$^-$ cells.

(D) Unsupervised clustering and heatmap of 127 genes whose expression is ≥2-fold higher in normal human CD34$^+$CD38$^+$CD10$^+$ B cell progenitors as compared to normal human CD34$^+$CD38$^-$ CB cells (Hystad et al., 2007) showing their relative expression (*Z* score) in CD34$^+$CD38$^-$ cells.

*p < 0.05.

In the GM lineages, the observed enhancing effect of IK6 expression on human cells could be traced to several specific stages of GM progenitors and was associated with a selectively increased sensitivity to two granulopoietic growth factors, IL-3 and GM-CSF. These cytokines share a common signaling receptor component and hence activate many common downstream intermediates (Gubina et al., 2001). Hyperactivation of the transcription factor CREB, and its downstream targets FOS and Cyclin B1, was also revealed, consistent with a role of IKAROS in normally

(E) Representative flow cytometric plots of lymphoid progenitor (CD34$^+$CD38$^+$CD10$^+$) cells from NSG mice cotransplanted 10 weeks previously with IK6- and control-transduced cells and then stained for intracellular Cyclin B1 protein.

(F) Percent Cyclin B1$^+$ human cells in NSG mice cotransplanted with IK6- and control-transduced cells 10 weeks previously (mean ± SEM; four mice).

MFI, median fluorescent intensity; *p < 0.05.

inhibiting the proliferation of primitive human hematopoietic cells. In agreement with previous findings (Dijon et al., 2008), an opposite effect on erythropoietic cells was noted.

In summary, we provide multiple lines of evidence for a stimulatory role of IK6 in primitive normal human hematopoietic cells, associated with an enhanced activation of certain signaling intermediates involved in GM-CSF and IL-3 responses. This finding, reinforced by the demonstration of IKAROS protein expression in all known stages of primitive human hematopoietic cells, strongly implicates IKAROS as a cell-intrinsic negative regulator of HSCs and their immediate progeny in humans. However, none of these sequelae appear sufficient to lead to the induction of leukemia in human cells, suggesting that mutations targeting *IKZF1* require additional alterations in order to produce such an outcome.

EXPERIMENTAL PROCEDURES

Lentiviral Constructs

Human IK6 cDNA was cloned into a pCCL.PPT.MNDU3.PGK.GFP lentiviral vector (Carbonaro et al., 2006; Challita et al., 1995) and sequence verified. IK6-GFP and control (empty)-YFP lentivirus was produced and concentrated as described previously (Imren et al., 2004). Titration on HeLa cells gave titers of $\sim 10^7$ infectious units/ml.

Mouse Transplantations

C57BL/6J -*Ly5.2* (B6) mice were used as donors and congenic B6-*W*^{41}/*W*^{41}-*Ly5.1* mice (given 400 cGy) or allogeneic NSG or NSG-3GS mice (given 315 cGy) were used as recipients. All mice were bred and maintained in the BC Cancer Research Animal Resource Centre under specific-pathogen-free conditions in accordance with Canadian Council on Animal Care guidelines and with approval from the Animal Care Committee of the University of British Columbia. LSK BM cells were transduced for 4 hr as described previously (Copley et al., 2013) (see Supplemental Experimental Procedures) and equal numbers of control and IK6-virus-exposed cells then immediately coinjected intravenously into recipients (1.5×10^4 cells each/mouse). For secondary transplants of mouse cells, pooled BM cells from both femurs and tibiae and the pelvis of each primary recipient were injected intravenously into two secondary mice and blood chimerism ascertained as described previously (Copley et al., 2013).

Human Cells

CD34$^+$ cell-enriched CB populations (>85% pure) were isolated by EasySep (STEMCELL Technologies) and transduced as previously described previously (Imren et al., 2004) using a 16 hr prestimulation and 8 hr virus exposure protocol (see Supplemental Experimental Procedures). For xenografts, primary mice were cotransplanted with equal aliquots of 1–5 $\times$ 10^5 control- and IK6-transduced cells without further selection. For secondary transplants, pooled BM cells from both femurs, tibiae and the pelvis of each primary recipient were injected intravenously into one or more secondary mice with or without prior selection by fluorescence-activated cell sorting (FACS) of human CD34$^+$CD38$^-$ cells, as indicated. Analysis of chimerism was performed as previously described (Cheung et al., 2012); unstained GFP$^+$ and YFP$^+$ cells from the same mice were used as negative (unstained) controls. For in vitro experiments, cells were cultured for 40 hr posttransduction prior to selection of GFP/YFP$^+$ cells by FACS. All procedures were carried according to protocols approved by the University of British Columbia research ethics board.

Western Blotting

Transduced (GFP$^+$ and YFP$^+$) CD34$^+$ CB cells were isolated by FACS 48 hr after viral exposure, lysed, resolved on a 4%–12% Bis-Tris (SDS) polyacrylamide gel, and transferred to Immobilon-P Transfer Membrane (Millipore), then immunoblotted with rabbit anti-IKAROS and histone H3 antibodies (Cell Signaling Technologies). Proteins were detected by horseradish peroxidase-conjugated anti-rabbit antibody (Santa Cruz Biotechnology) and Supersignal Femto Maximum Sensitivity Reagent (Pierce Biotechnology). Non-saturating signals were acquired using a VersaDoc system (Bio-Rad) and quantitated using ImageLab version 3 (Bio-Rad).

Confocal Imaging

Transduced CD34$^+$ CB cells were prepared as for intracellular flow cytometry then cytospun onto coated slides. Slides were mounted with Vectashield containing DAPI (VECTOR Laboratories). Images were acquired with a FluoView confocal laser scanning microscope (Fv10i, Olympus) and processed with ImageJ.

Intracellular Flow Cytometric Analyses

See Supplemental Experimental Procedures for details regarding intracellular flow cytometric analyses.

Cell Cultures

CFC assays and LTCs were performed as described previously (Hogge et al., 1996), using for the LTCs a mixture of irradiated M210B4 and *Sl/Sl* mouse stromal cells producing human SF, IL-3, FL, and G-CSF. Live (propidium iodide negative [PI$^-$]) nonadherent cells were enumerated by flow cytometry using fluorescent counting beads (AccuCheck, Life Technologies) and their morphology determined on Wright-Giemsa-stained cytospin preparations. For suspension culture experiments, test cells were incubated in either serum-free medium (SFM) with growth factors (as for lentiviral exposure; Figures 4H–4J) or H5100 media with GM-CSF (Figure S3C).

To compare the cytokine sensitivity of IK6- and control-transduced lineage-SCA-1$^+$CD3$^-$ B6 mouse BM cells, 10^4 of each were cocultured in 100 μl SFM in 96-well plates with added mouse SF or IL-3, as indicated. After 4 days, total viable (PI$^-$) GFP$^+$ and YFP$^+$ cells in each well were enumerated by flow cytometry using fluorescent counting beads.

qRT-PCR

RNA was prepared using spin columns (QIAGEN) and cDNA using SuperScript VILO (Life Technologies). Primers for qRT-PCR were

designed to amplify across at least one intron and produce a product of 80–100 bp using Primer3 software (http://frodo.wi.mit.edu/). qRT-PCR reactions were performed using Fast SYBR green (Life Technologies) and a 7500 Fast Real-Time PCR analyzer (Applied Biosystems). Transcripts were normalized to *ABL1* and/or *B2M* as indicated and the mean ΔCt values used to generate ratios of transcript levels in IK6 versus control cells.

Statistical Analysis

IK6 and control-transduced cell outputs were compared using the Student's t test (paired or unpaired as appropriate). IL-3 and GM-CSF surface receptor expression was compared by unbiased analysis of flow cytometry data using the flowType and RchyOptimyx algorithms (Aghaeepour et al., 2012a; Aghaeepour et al., 2012b).

Gene Expression Analysis

See Supplemental Experimental Procedures for details regarding gene expression analysis.

ACCESSION NUMBERS

The NCBI Gene Expression Omnibus accession number for the gene expression array data reported in this paper is GSE60957.

SUPPLEMENTAL INFORMATION

Supplemental Information includes Supplemental Experimental Procedures, four figures, and two tables and can be found with this article online at http://dx.doi.org/10.1016/j.stemcr.2014.09.006.

AUTHOR CONTRIBUTIONS

P.A.B. designed and performed experiments, analyzed data and wrote the manuscript. D.J.H.F.K. analyzed gene expression profiling data. N.K. performed confocal microscopy. D.J.H.F.K. and L.W. optimized phosphoflow cytometry protocols. P.H.M. and G.R. performed and optimized xenograft analyses and animal husbandry protocols. N.A. performed bioinformatic analysis of flow cytometry data. S.B., K.S., and S.R. performed cloning and western blotting. E.B. performed cell culture experiments. C.J.E. directed the project and cowrote the manuscript.

ACKNOWLEDGMENTS

We thank Glen Edin and Margaret Hale and the Flow Cytometry Core Facility and Animal Resource Center of the BC Cancer Agency for technical assistance. We are also grateful to Bertie Göttgens and Mark Dawson (University of Cambridge, UK) for sharing human STAT5 target gene data. This work was supported by grants from the Terry Fox Foundation, the Canadian Institutes of Health Research (CIHR), and the Natural Sciences and Engineering Research Council of Canada. P.A.B. held a Kay Kendall Leukaemia Fund Intermediate Fellowship from the UK. D.J.H.F.K. held a Vanier Canada Graduate Scholarship. P.M. holds a CIHR Banting Studentship, and S.B. held a University of British Columbia Graduate Studentship and a Vanier Canada Graduate Scholarship. E.B. held a CIHR Training Program in Regenerative Medicine Fellowship.

Received: March 18, 2014
Revised: September 8, 2014
Accepted: September 8, 2014
Published: October 9, 2014

REFERENCES

Aghaeepour, N., Chattopadhyay, P.K., Ganesan, A., O'Neill, K., Zare, H., Jalali, A., Hoos, H.H., Roederer, M., and Brinkman, R.R. (2012a). Early immunologic correlates of HIV protection can be identified from computational analysis of complex multivariate T-cell flow cytometry assays. Bioinformatics *28*, 1009–1016.

Aghaeepour, N., Jalali, A., O'Neill, K., Chattopadhyay, P.K., Roederer, M., Hoos, H.H., and Brinkman, R.R. (2012b). RchyOptimyx: cellular hierarchy optimization for flow cytometry. Cytometry A *81*, 1022–1030.

Billerbeck, E., Barry, W.T., Mu, K., Dorner, M., Rice, C.M., and Ploss, A. (2011). Development of human CD4+FoxP3+ regulatory T cells in human stem cell factor-, granulocyte-macrophage colony-stimulating factor-, and interleukin-3-expressing NOD-SCID IL2Rγ(null) humanized mice. Blood *117*, 3076–3086.

Carbonaro, D.A., Jin, X., Petersen, D., Wang, X., Dorey, F., Kil, K.S., Aldrich, M., Blackburn, M.R., Kellems, R.E., and Kohn, D.B. (2006). In vivo transduction by intravenous injection of a lentiviral vector expressing human ADA into neonatal ADA gene knockout mice: a novel form of enzyme replacement therapy for ADA deficiency. Mol. Ther. *13*, 1110–1120.

Challita, P.M., Skelton, D., el-Khoueiry, A., Yu, X.J., Weinberg, K., and Kohn, D.B. (1995). Multiple modifications incis elements of the long terminal repeat of retroviral vectors lead to increased expression and decreased DNA methylation in embryonic carcinoma cells. J. Virol. *69*, 748–755.

Cheung, A.M., Leung, D., Rostamirad, S., Dhillon, K., Miller, P.H., Droumeva, R., Brinkman, R.R., Hogge, D., Roy, D.C., and Eaves, C.J. (2012). Distinct but phenotypically heterogeneous human cell populations produce rapid recovery of platelets and neutrophils after transplantation. Blood *119*, 3431–3439.

Conley, M.E., Rohrer, J., Rapalus, L., Boylin, E.C., and Minegishi, Y. (2000). Defects in early B-cell development: comparing the consequences of abnormalities in pre-BCR signaling in the human and the mouse. Immunol. Rev. *178*, 75–90.

Copley, M.R., Babovic, S., Benz, C., Knapp, D.J., Beer, P.A., Kent, D.G., Wohrer, S., Treloar, D.Q., Day, C., Rowe, K., et al. (2013). The Lin28b-let-7-Hmga2 axis determines the higher self-renewal potential of fetal haematopoietic stem cells. Nat. Cell Biol. *15*, 916–925.

Dawson, M.A., Foster, S.D., Bannister, A.J., Robson, S.C., Hannah, R., Wang, X., Xhemalce, B., Wood, A.D., Green, A.R., Göttgens, B., and Kouzarides, T. (2012). Three distinct patterns of histone H3Y41 phosphorylation mark active genes. Cell Reports *2*, 470–477.

Dijon, M., Bardin, F., Murati, A., Batoz, M., Chabannon, C., and Tonnelle, C. (2008). The role of Ikaros in human erythroid differentiation. Blood *111*, 1138–1146.

Doulatov, S., Notta, F., Laurenti, E., and Dick, J.E. (2012). Hematopoiesis: a human perspective. Cell Stem Cell *10*, 120–136.

Eppert, K., Takenaka, K., Lechman, E.R., Waldron, L., Nilsson, B., van Galen, P., Metzeler, K.H., Poeppl, A., Ling, V., Beyene, J., et al. (2011). Stem cell gene expression programs influence clinical outcome in human leukemia. Nat. Med. *17*, 1086–1093.

Ferreirós-Vidal, I., Carroll, T., Taylor, B., Terry, A., Liang, Z., Bruno, L., Dharmalingam, G., Khadayate, S., Cobb, B.S., Smale, S.T., et al. (2013). Genome-wide identification of Ikaros targets elucidates its contribution to mouse B-cell lineage specification and pre-B-cell differentiation. Blood *121*, 1769–1782.

Grossmann, V., Kohlmann, A., Zenger, M., Schindela, S., Eder, C., Weissmann, S., Schnittger, S., Kern, W., Müller, M.C., Hochhaus, A., et al. (2011). A deep-sequencing study of chronic myeloid leukemia patients in blast crisis (BC-CML) detects mutations in 76.9% of cases. Leukemia *25*, 557–560.

Gubina, E., Luo, X., Kwon, E., Sakamoto, K., Shi, Y.F., and Mufson, R.A. (2001). betac cytokine receptor-induced stimulation of cAMP response element binding protein phosphorylation requires protein kinase C in myeloid cells: a novel cytokine signal transduction cascade. J. Immunol. *167*, 4303–4310.

Hogge, D.E., Lansdorp, P.M., Reid, D., Gerhard, B., and Eaves, C.J. (1996). Enhanced detection, maintenance, and differentiation of primitive human hematopoietic cells in cultures containing murine fibroblasts engineered to produce human steel factor, interleukin-3, and granulocyte colony-stimulating factor. Blood *88*, 3765–3773.

Hu, Y., and Smyth, G.K. (2009). ELDA: extreme limiting dilution analysis for comparing depleted and enriched populations in stem cell and other assays. J. Immunol. Methods *347*, 70–78.

Hystad, M.E., Myklebust, J.H., Bø, T.H., Sivertsen, E.A., Rian, E., Forfang, L., Munthe, E., Rosenwald, A., Chiorazzi, M., Jonassen, I., et al. (2007). Characterization of early stages of human B cell development by gene expression profiling. J. Immunol. *179*, 3662–3671.

Iacobucci, I., Lonetti, A., Messa, F., Cilloni, D., Arruga, F., Ottaviani, E., Paolini, S., Papayannidis, C., Piccaluga, P.P., Giannoulia, P., et al. (2008). Expression of spliced oncogenic Ikaros isoforms in Philadelphia-positive acute lymphoblastic leukemia patients treated with tyrosine kinase inhibitors: implications for a new mechanism of resistance. Blood *112*, 3847–3855.

Imren, S., Fabry, M.E., Westerman, K.A., Pawliuk, R., Tang, P., Rosten, P.M., Nagel, R.L., Leboulch, P., Eaves, C.J., and Humphries, R.K. (2004). High-level beta-globin expression and preferred intragenic integration after lentiviral transduction of human cord blood stem cells. J. Clin. Invest. *114*, 953–962.

Jäger, R., Gisslinger, H., Passamonti, F., Rumi, E., Berg, T., Gisslinger, B., Pietra, D., Harutyunyan, A., Klampfl, T., Olcaydu, D., et al. (2010). Deletions of the transcription factor Ikaros in myeloproliferative neoplasms. Leukemia *24*, 1290–1298.

Joshi, I., Yoshida, T., Jena, N., Qi, X., Zhang, J., Van Etten, R.A., and Georgopoulos, K. (2014). Loss of Ikaros DNA-binding function confers integrin-dependent survival on pre-B cells and progression to acute lymphoblastic leukemia. Nat. Immunol. *15*, 294–304.

Lopez, R.A., Schoetz, S., DeAngelis, K., O'Neill, D., and Bank, A. (2002). Multiple hematopoietic defects and delayed globin switching in Ikaros null mice. Proc. Natl. Acad. Sci. USA *99*, 602–607.

Ma, S., Pathak, S., Mandal, M., Trinh, L., Clark, M.R., and Lu, R. (2010). Ikaros and Aiolos inhibit pre-B-cell proliferation by directly suppressing c-Myc expression. Mol. Cell. Biol. *30*, 4149–4158.

Malinge, S., Thiollier, C., Chlon, T.M., Doré, L.C., Diebold, L., Bluteau, O., Mabialah, V., Vainchenker, W., Dessen, P., Winandy, S., et al. (2013). Ikaros inhibits megakaryopoiesis through functional interaction with GATA-1 and NOTCH signaling. Blood *121*, 2440–2451.

Mestas, J., and Hughes, C.C. (2004). Of mice and not men: differences between mouse and human immunology. J. Immunol. *172*, 2731–2738.

Miller, P.H., Cheung, A.M., Beer, P.A., Knapp, D.J., Dhillon, K., Rabu, G., Rostamirad, S., Humphries, R.K., and Eaves, C.J. (2013). Enhanced normal short-term human myelopoiesis in mice engineered to express human-specific myeloid growth factors. Blood *121*, e1–e4.

Mullighan, C.G., Miller, C.B., Radtke, I., Phillips, L.A., Dalton, J., Ma, J., White, D., Hughes, T.P., Le Beau, M.M., Pui, C.H., et al. (2008). BCR-ABL1 lymphoblastic leukaemia is characterized by the deletion of Ikaros. Nature *453*, 110–114.

Nacheva, E.P., Grace, C.D., Brazma, D., Gancheva, K., Howard-Reeves, J., Rai, L., Gale, R.E., Linch, D.C., Hills, R.K., Russell, N., et al. (2013). Does BCR/ABL1 positive acute myeloid leukaemia exist? Br. J. Haematol. *161*, 541–550.

Nakayama, H., Ishimaru, F., Avitahl, N., Sezaki, N., Fujii, N., Nakase, K., Ninomiya, Y., Harashima, A., Minowada, J., Tsuchiyama, J., et al. (1999). Decreases in Ikaros activity correlate with blast crisis in patients with chronic myelogenous leukemia. Cancer Res. *59*, 3931–3934.

Nichogiannopoulou, A., Trevisan, M., Neben, S., Friedrich, C., and Georgopoulos, K. (1999). Defects in hemopoietic stem cell activity in Ikaros mutant mice. J. Exp. Med. *190*, 1201–1214.

Notta, F., Doulatov, S., Laurenti, E., Poeppl, A., Jurisica, I., and Dick, J.E. (2011). Isolation of single human hematopoietic stem cells capable of long-term multilineage engraftment. Science *333*, 218–221.

Novershtern, N., Subramanian, A., Lawton, L.N., Mak, R.H., Haining, W.N., McConkey, M.E., Habib, N., Yosef, N., Chang, C.Y., Shay, T., et al. (2011). Densely interconnected transcriptional circuits control cell states in human hematopoiesis. Cell *144*, 296–309.

Papathanasiou, P., Attema, J.L., Karsunky, H., Hosen, N., Sontani, Y., Hoyne, G.F., Tunningley, R., Smale, S.T., and Weissman, I.L. (2009). Self-renewal of the long-term reconstituting subset of hematopoietic stem cells is regulated by Ikaros. Stem Cells *27*, 3082–3092.

Payne, K.J., and Crooks, G.M. (2007). Immune-cell lineage commitment: translation from mice to humans. Immunity *26*, 674–677.

Payne, K.J., and Dovat, S. (2011). Ikaros and tumor suppression in acute lymphoblastic leukemia. Crit. Rev. Oncog. *16*, 3–12.

Rangarajan, A., and Weinberg, R.A. (2003). Opinion: Comparative biology of mouse versus human cells: modelling human cancer in mice. Nat. Rev. Cancer *3*, 952–959.

Ross, J., Mavoungou, L., Bresnick, E.H., and Milot, E. (2012). GATA-1 utilizes Ikaros and polycomb repressive complex 2 to

suppress Hes1 and to promote erythropoiesis. Mol. Cell. Biol. *32*, 3624–3638.

Schwickert, T.A., Tagoh, H., Gültekin, S., Dakic, A., Axelsson, E., Minnich, M., Ebert, A., Werner, B., Roth, M., Cimmino, L., et al. (2014). Stage-specific control of early B cell development by the transcription factor Ikaros. Nat. Immunol. *15*, 283–293.

Sun, L., Heerema, N., Crotty, L., Wu, X., Navara, C., Vassilev, A., Sensel, M., Reaman, G.H., and Uckun, F.M. (1999). Expression of dominant-negative and mutant isoforms of the antileukemic transcription factor Ikaros in infant acute lymphoblastic leukemia. Proc. Natl. Acad. Sci. USA *96*, 680–685.

Theocharides, A.P., Dobson, S.M., Laurenti, E., Notta, F., Voisin, V., Cheng, P.Y., Yuan, J.S., Guidos, C.J., Minden, M.D., Mullighan, C.G., et al. (2014). Dominant-negative Ikaros cooperates with BCR-ABL1 to induce human acute myeloid leukemia in xenografts. Leukemia. Published online May 5, 2014. http://dx.doi.org/10.1038/leu.2014.150.

Tonnelle, C., Bardin, F., Maroc, C., Imbert, A.M., Campa, F., Dalloul, A., Schmitt, C., and Chabannon, C. (2001). Forced expression of the Ikaros 6 isoform in human placental blood CD34(+) cells impairs their ability to differentiate toward the B-lymphoid lineage. Blood *98*, 2673–2680.

Tonnelle, C., Dijon, M., Moreau, T., Garulli, C., Bardin, F., and Chabannon, C. (2009). Stage specific over-expression of the dominant negative Ikaros 6 reveals distinct role of Ikaros throughout human B-cell differentiation. Mol. Immunol. *46*, 1736–1743.

Zhang, X., Odom, D.T., Koo, S.H., Conkright, M.D., Canettieri, G., Best, J., Chen, H., Jenner, R., Herbolsheimer, E., Jacobsen, E., et al. (2005). Genome-wide analysis of cAMP-response element binding protein occupancy, phosphorylation, and target gene activation in human tissues. Proc. Natl. Acad. Sci. USA *102*, 4459–4464.

Zhang, J., Jackson, A.F., Naito, T., Dose, M., Seavitt, J., Liu, F., Heller, E.J., Kashiwagi, M., Yoshida, T., Gounari, F., et al. (2012). Harnessing of the nucleosome-remodeling-deacetylase complex controls lymphocyte development and prevents leukemogenesis. Nat. Immunol. *13*, 86–94.

Stem Cell Reports, Volume *3*

Supplemental Information

A Dominant-Negative Isoform of IKAROS Expands Primitive Normal Human Hematopoietic Cells

Philip A. Beer, David J.H.F. Knapp, Nagarajan Kannan, Paul H. Miller, Sonja Babovic, Elizabeth Bulaeva, Nima Aghaeepour, Gabrielle Rabu, Shabnam Rostamirad, Kingsley Shih, Lisa Wei, and Connie J. Eaves

Supplemental Methods

Protocol for lentiviral gene transfer

For lentiviral transduction of mouse BM cells, sorted LSK cells were resuspended in serum-free medium (SFM = IMDM containing BIT^{TM} plus 40 μg/mL low-density lipoproteins from STEMCELL Technologies and 10^{-4} M 2-mercaptoethanol from Sigma) and then exposed to concentrated lentivirus for 4 hours in the presence of added mouse SF (STEMCELL) and IL-11 (Genetics Institute) at final concentrations of 300 ng/ml and 20 ng/ml, respectively.

For lentiviral transduction of human CB cells, purified $CD34^+$ cells or subsets thereof were stimulated overnight (~16 hours) at 1 to 10 $x10^5$ cells/ml in SFM containing 100 ng/ml recombinant human FL (Immunex Corp.) and SF (STEMCELL), plus 20 ng/ml IL-3 (Novartis), IL-6 (Cangene) and G-CSF (STEMCELL) and then exposed to lentivirus for another 8 hours in the same medium.

Intracellular flow cytometric analyses

For detection of intracellular proteins (IKAROS, FOS or CCNB1), cells were fixed with 1.6% paraformaldehyde, detergent permeabilized (eBioscience), incubated with blocking reagent (PBS with 2% fetal bovine serum, 5% human AB serum and anti-human CD32 antibody clone IV.3) and then stained with surface and intracellular antibodies (rabbit anti-IKAROS, FOS or CCNB1; Cell Signaling Technologies) followed by AlexaFluor-594-labelled anti-rabbit secondary (Invitrogen). For detection of intracellular signaling molecules, cells were washed twice in IMDM and then incubated for 3 hours at 37^{o}C without serum or growth factors. Cells were then stimulated (or not) for 10 minutes at 37^{o}C, fixed with 1.6% paraformaldehyde, washed twice, incubated on ice with

blocking reagent, incubated with antibodies against surface antigens, washed twice, then resuspended in 80% ethanol at -80^{o}C, followed immediately by 2 washes. Cells from different conditions were differentially labeled with combinations of amine reactive dyes (Pacific Blue and eFluor 506 and 780, eBioscience), washed twice and combined for staining on ice with intracellular antibodies (AKT pS473, ERK1/2 pT202/pY204, P38 MAPK pT180/pY182, STAT1 pY701, STAT3 pY705 and STAT5 pY694, BD; CREB pS133 and JAK2 pY1008, Cell Signaling Technologies), followed by washing and staining with appropriate secondary antibodies. Cells harvested from mice were first incubated in NH_4Cl, then processed as above without an initial incubation in the absence of serum or growth factors and with the addition of anti-mouse CD16/CD32 clone 2.4G2 to the blocking reagent. All flow cytometry analyses were performed on a Fortessa (BD) and data analyzed using FlowJo software (Tree Star). GFP^+ and YFP^+ cells stained with surface antibodies and labeled with amine reactive dyes (where used) but not with intracellular antibodies were used as negative (unstained) controls.

Gene expression analysis

Global transcriptome data was obtained from 3 biological replicates of purified $CD34^+CD38^-$ cells isolated from 3 mice transplanted 10 weeks previously. RNA quality was assessed using an Agilent 2100 bioanalyzer (acceptable RIN value $\geq$8.0), labeled using the Agilent One-Color Microarray-Based Exon Analysis Low Input Quick Amp WT Labeling v1.0 and then hybridized to Agilent Human GE 8x60K arrays. Data were acquired using an Agilent DNA Microarray Scanner at a 3 mm scan resolution, and processed with Agilent Feature Extraction 11.0.1.1. Probes were retained if detectable in all control or all IK6 samples and had an EntrezGene identifier. Following trimming, data were analyzed using R software. Raw signals were quantile normalized and

differential expression tested per-probe (lmFit, limma) or within gene sets (romer, limma with 10^6 rotations using floormean) using the 'KEGG' and 'transcription factor targets (TRANSFAC)' gene sets from MSigDB version 4, and specific gene lists as indicated, with correction for multiple testing (qvalue). STAT5 targets were derived from the human HEL cell line by intersecting STAT5 ChIP-Seq data with gene expression profiling with and without JAK2 inhibition ((Dawson et al., 2012), courtesy of Bertie Göttgens and Mark Dawson). The NCBI Gene Expression Omnibus accession number for the gene expression array data reported in this paper is GSE60957.

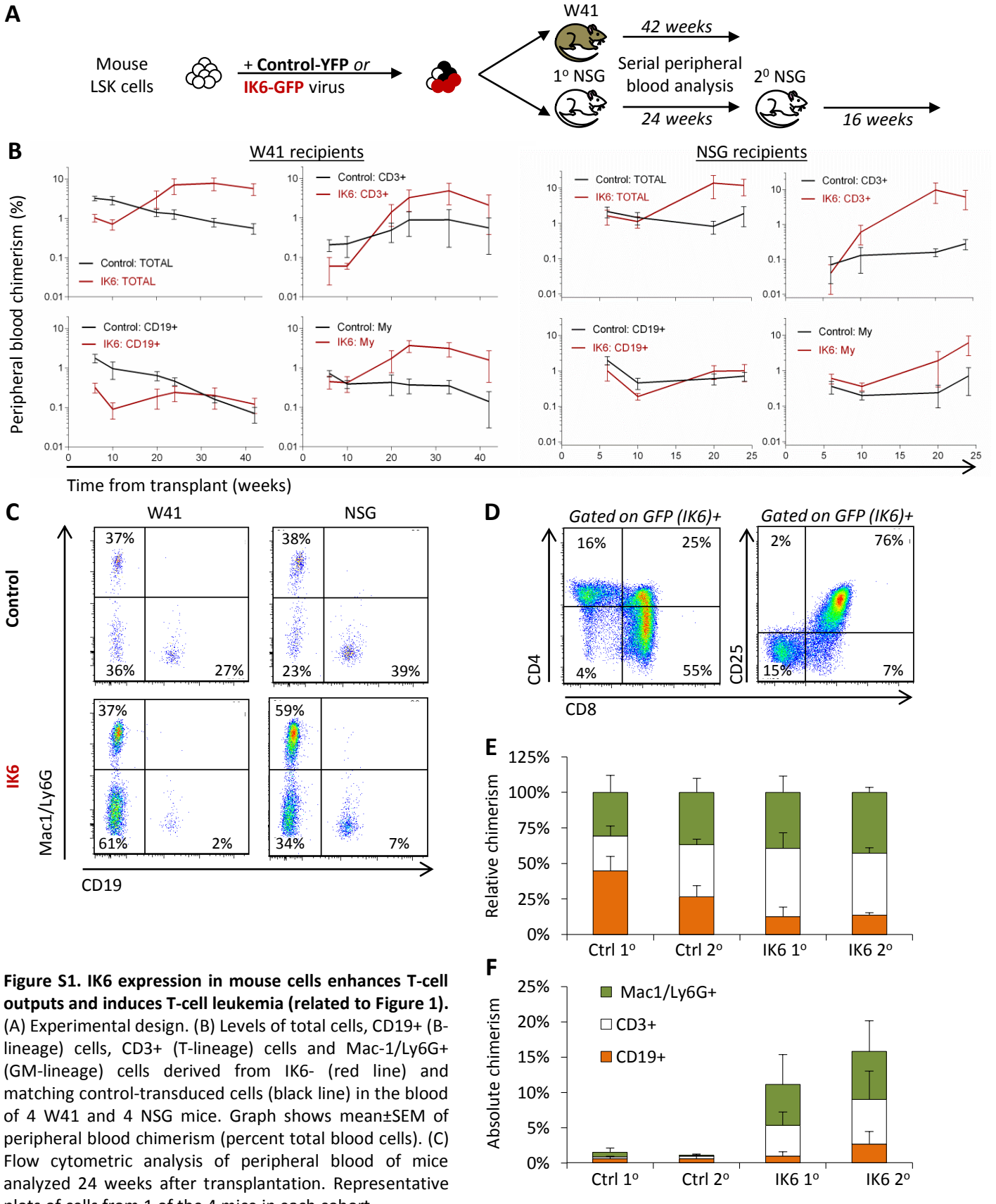

Figure S1. IK6 expression in mouse cells enhances T-cell outputs and induces T-cell leukemia (related to Figure 1). (A) Experimental design. (B) Levels of total cells, CD19+ (B-lineage) cells, CD3+ (T-lineage) cells and Mac-1/Ly6G+ (GM-lineage) cells derived from IK6- (red line) and matching control-transduced cells (black line) in the blood of 4 W41 and 4 NSG mice. Graph shows mean±SEM of peripheral blood chimerism (percent total blood cells). (C) Flow cytometric analysis of peripheral blood of mice analyzed 24 weeks after transplantation. Representative plots of cells from 1 of the 4 mice in each cohort. (D) Representative flow cytometric analysis of peripheral blood of 1 of 3 mice who developed aggressive T-ALL 18-34 weeks after initial transplantation. Transplantation of primary leukemias resulted in rapid (<3 weeks) death of secondary recipients. (E&F) Relative and absolute lineage contribution from control and IK6-transduced cells in 24-week primary (1º) NSG mice and 16-week secondary (2º) NSG mice. Graph shows mean±SEM for 4 primary and 7 secondary mice.

A

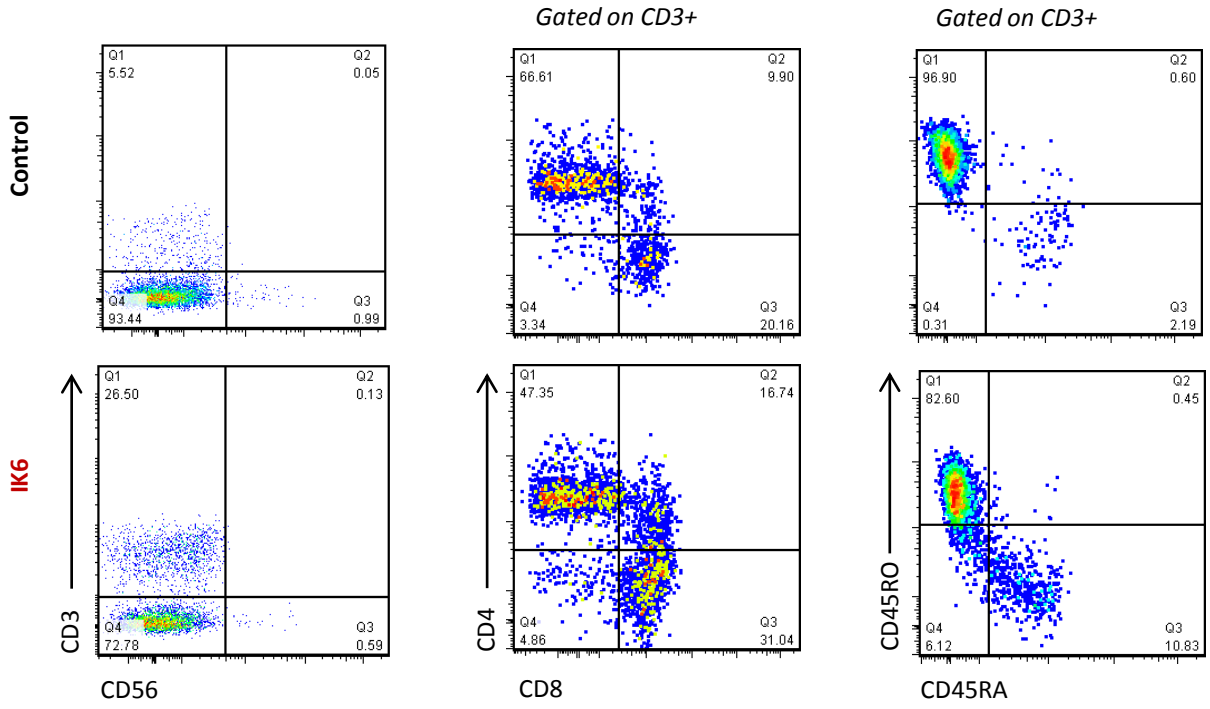

B

	CD3+CD4+		CD3+CD8+		CD3+CD45RA+		CD3-CD56+	
	Control	**IK6**	**Control**	**IK6**	**Control**	**IK6**	**Control**	**IK6**
Mean chimerism	1.08%	0.54%	0.14%	0.57%	0.03%	0.12%	0.46%	0.34%
Standard error	0.42%	0.38%	0.08%	0.53%	0.003%	0.09%	0.23%	0.07%
No. of mice	3		3		3		8	
T-test (paried)	0.53		0.51		0.46		0.40	

Figure S2. Effects of IK6 expression on human T- and NK-cell differentiation (related to Figure 2). (A) Representative flow cytometric profiles of IK6- and control-derived NK- and T-cells from the spleens of 10-week transplanted NSG-3GS mice, as shown in Figure 2F. (B) Human IK6- and control-derived T-cells subsets in the spleens of 10-week transplanted NSG-3G3 mice, expressed a percentage of the total number of cells in the spleen.

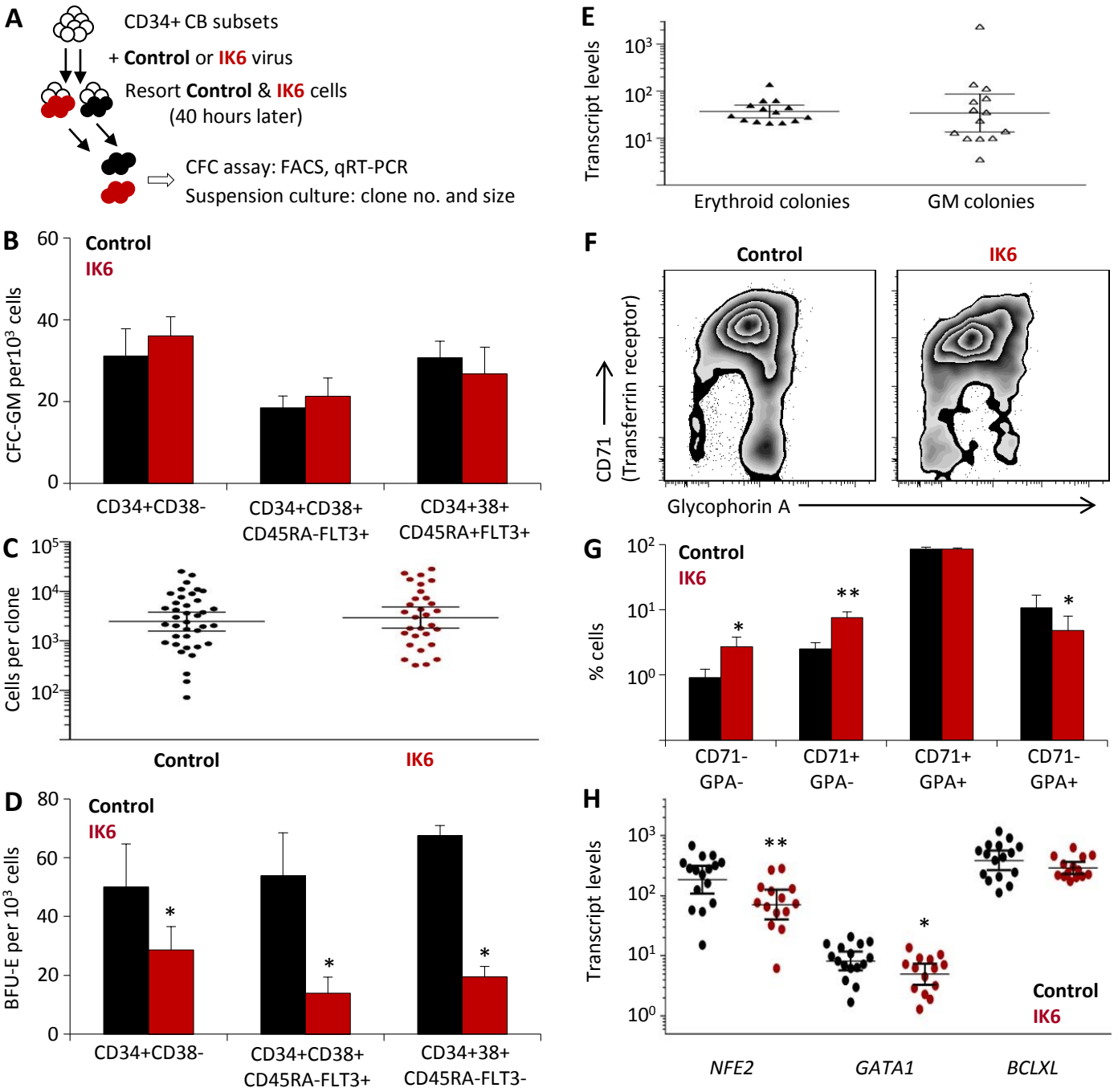

Figure S3. Opposite effects of IK6 on human CB cell-derived granulopoiesis and erythropoiesis (related to Figure 4). (A) Experimental design. (B) Lack of effect of IK6 on GM colony formation by different subsets of CD34$^+$ CB cells (x-axis) assessed directly post-transduction (mean±SEM, 3 experiments). (C) Lack of effect of IK6 on the size of clones (produced after 14 days in H5100 LTC medium with 20 ng/mL GM-CSF) from transduced CD34$^+$CD38$^-$ cells (mean±SEM). Frequency of clone formation was also similar at 16% (30/188) and 20% (38/188) for IK6- and control-transduced cells, respectively. (D) Colony formation by control- and IK6-transduced BFU-E present in different subsets of CD34$^+$ CB cells (x-axis) assessed immediately after transduction (mean±SEM, same experiments as in panel B). (E) IK6 transcript levels (relative to *B2M* expression) in 14 erythroid and 14 GM colonies generated *in vitro* from IK6-transduced cells (mean±SEM). (F) Representative flow cytometric profiles showing effects of IK6 on transferrin receptor and glycophorin A expression in erythroid cells generated after 14 days from IK6-transduced BFU-Es (1 of 5 such analyses performed on colonies produced in 2 experiments). (G) IK6 alters the proportion of erythroid cells at different stages of maturation (mean±SEM from 5 analyses). (H) IK6 has a slight effect in decreasing *NFE2* and *GATA1* transcripts in erythroid colonies - 14 IK6-derived and 14 controls assessed individually and genotyped by detection (or not) of IK6 transcripts (data not shown). Values are the mean±SEM. CD34$^+$CD38$^-$: multipotent progenitor; CD34$^+$CD38$^+$CD45RA$^-$FLT3$^+$: myloerythroid progenitor; CD34$^+$CD38$^+$CD45RA$^-$FLT3$^-$: erythroid progenitor; CD34$^+$CD38$^+$CD45RA$^+$FLT3$^+$: GM progenitor; CFC-GM: colony-forming cell-granulocyte-macrophage; BFU-E: burst-forming unit-erythroid; GPA: Glycophorin A; *: p=<0.05; **: p=<0.01.

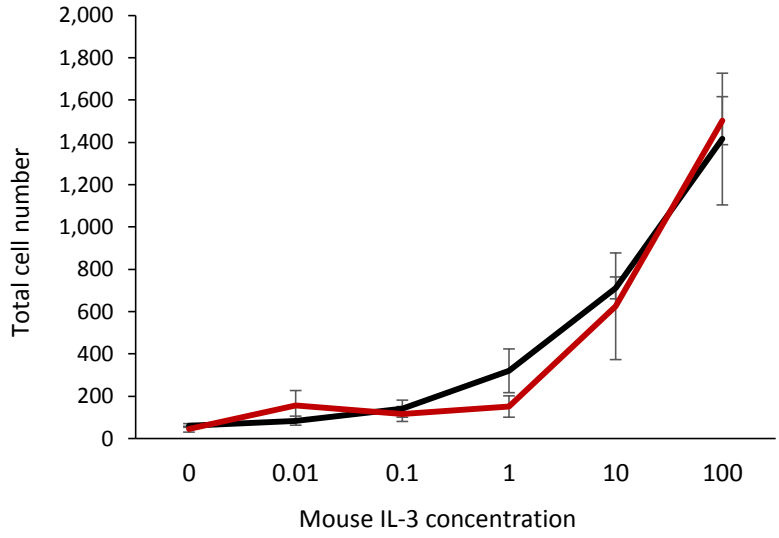

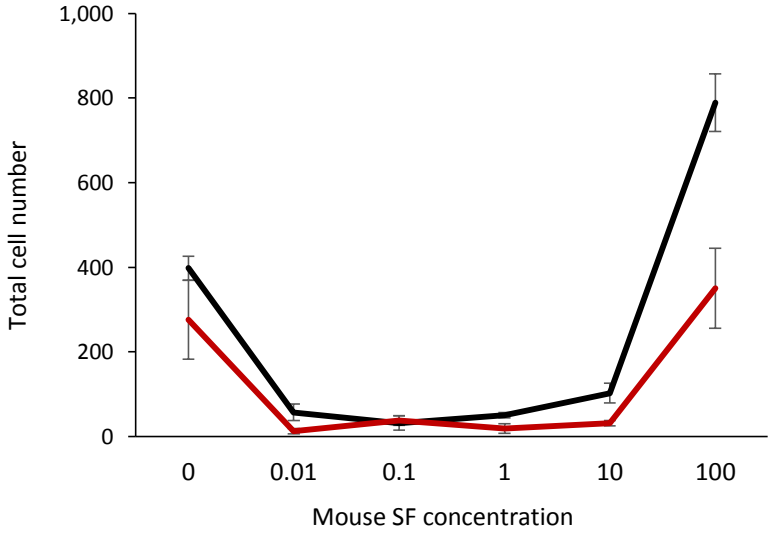

Figure S4. Forced expression of IK6 in primitive mouse hematopoietic cells does not alter their growth factor responsiveness (related to Figure 5). Day 4 cell outputs from IK6- and control-transduced mouse progenitor cells ($Lin^{-}Sca1^{+}CD3^{-}$) cultured in varying concentrations of IL-3 or Steel factor (SF). Figure shows mean±SEM of 3 replicates derived from 1 of 3 independent experiments, all of which showed similar results.